UNIVERSITÄTSKLINIKUM HAMBURG-EPPENDORF

Klinik und Poliklinik für Augenheilkunde, Experimentelle Ophthalmologie,
Universitätsklinikum Hamburg-Eppendorf

Prof. Dr. Martin Spitzer

Neural stem cell-based GDNF and CNTF for the treatment of retinal degeneration in a mouse model of CLN7 disease

Dissertation

zur Erlangung des Grades eines Doktors der Medizin
an der Medizinischen Fakultät der Universität Hamburg.

vorgelegt von:

Yingying Wei
aus Anhui

Hamburg 2022

Angenommen von der
Medizinischen Fakultät der Universität Hamburg am: 20.07.2022

Veröffentlicht mit Genehmigung der
Medizinischen Fakultät der Universität Hamburg.

Prüfungsausschuss, der/die Vorsitzende: PD Dr. Christian Bernreuther

Prüfungsausschuss, zweite/r Gutachter/in: Prof. Dr. Udo Bartsch

The eye is the window of the human body through which it feels its way and enjoys the beauty of the world. Owing to the eye the soul is content to stay in its bodily prison, for without it such bodily prison is torture.

Leonardo da Vinci (1452–1519)

Stem cell-based intravitreal delivery of GDNF and CNTF for the treatment of retinal degeneration in a mouse model of CLN7 disease

Stem cell-based intravitreal delivery of GDNF and CNTF for the treatment of retinal degeneration in a mouse model of CLN7 disease

1. Introduction

1.1 Neuronal ceroid lipofuscinosis (NCL)

Neuronal ceroid lipofuscinosis (NCL) is the umbrella term for a group of 13 genetically distinct lysosomal storage disorders. All NCLs are characterized by intracellular accumulation of lysosomal autofluorescent lipofuscin and progressive neurodegeneration in the brain and retina, leading to physical and mental disability, vision loss and eventually premature death (Boustany 2013; Kohlschutter et al. 2019; Gardner and Mole 2021). The incidence of NCL is estimated to be 1 to 4 in 100,000 live births (Dolisca et al. 2013; Haltia and Goebel 2013; Nita et al. 2016). NCLs are mainly autosomal-recessive, and classified according to the affected gene in CLN1-CLN8 and CLN10-CLN14 (Mole and Cotman 2015; Kohlschutter et al. 2019; Gardner and Mole 2021). To date, over 600 genetic mutations have been discovered as causes of NCL (https://www.ucl.ac.uk/ncl-disease/mutation-and-patient-database/mutation-and-patient-datasheets-human-ncl-genes [stand: 10.05.2020,22:50]).

1.2 CLN7

CLN7 disease with late infantile onset is caused by mutations in the major facilitator superfamily domain containing 8 (*MFSD8*) gene (Kousi et al. 2009). Up to now, 46 different mutations in the *MFSD8* gene have been identified leading to CLN7 disease with onset in late infancy or at later ages (https://www.ucl.ac.uk/ncl-disease/mutation-and-patient-database/mutation-and-patient-datasheets-human-ncl-genes/cln7-mfsd8 [stand:

10.05.2020,22:50]). Missense mutations account for about 70% of the pathogenic mutations in the *MFSD8* gene and occur across the gene's coding domain (Craiu et al. 2015; Kozina et al. 2018; Hosseini Bereshneh and Garshasbi 2018; Reith et al. 2022). CLN7 was identified as a novel endolysosomal chloride channel using a transgenic mouse model with a 3148 base pair (bp) deletion from the fourth to sixth exon of the *Mfsd8* gene. Located in lysosomes and endosomes, CLN7 regulates lysosomal chloride conductance, luminal pH, lysosomal membrane potential and promotes lysosomal Ca2+ release. As a result, pathogenic mutations in CLN7 result in a reduction in chloride permeability (Wang et al. 2021). In the *Cln7* knockout (ko) mouse model, abnormal overexpression of the pro-glycolytic enzyme 6-Phosphofructo-2-Kinase/Fructose-2,6-Biphosphatase 3 (PFKFB3) in neurons has been implicated in the brain pathology (Lopez-Fabuel et al. 2022).

Babies carrying pathogenic *MFSD8* mutations do not manifest any clinical symptoms at birth; however, between the ages of 2 and 7 years old, psychomotor regression or seizures are often the initial symptoms of the disease followed by rapid cognitive and motor decline, myoclonus, personality abnormalities, and blindness. Rapid progress is characteristic of the disease. An onset resembling Rett syndrome has also been described (Craiu et al. 2015). While visual failure is the initial symptom in some patients (Patino et al. 2014; Topcu et al. 2004; Kousi et al. 2009; Aldahmesh et al. 2009), progressive visual loss later during the course of the disease is among the typical symptoms of all CLN7 patients. In CLN7 patients with advanced retinal dystrophies, full field electroretinogram (ffERG) of both eyes recordings showed flat scotopic and photopic responses. Fundus autofluorescence (FAF) showed a broad ring of mild hyperautofluorescence throughout each paramacular area, and fundus photography showed discrete salt-and-pepper depigmented retinal pigment alterations throughout the retinal periphery of both eyes. In such patients, optical coherence tomography (OCT) revealed a profound loss of outer retinal layers (Magliyah et al. 2019). Interestingly, in rare cases mutations in *MFSD8* have been reported to cause non-syndromic macular dystrophy, indicating that the retina appears to be more sensitive to CLN7 dysfunction than other tissues (Zare-Abdollahi et al. 2019; Bauwens et al. 2020; Khan et al. 2017; Magliyah et al. 2019; Roosing et al. 2015; Poncet et al. 2022; Xiang et al. 2021).

A hypomorphic *Cln7* mouse model was generated by insertion of a lacZ gene-trap cassette between exons 1 and 2 (Damme et al. 2014). Protein analyses revealed the presence of residual CLN7 protein in this mutant, probably as a result of a low degree of exon 1 to exon 2 splicing. Mutant mice showed some defects also present in human patients with *MFSD8* mutations, such as dysregulation of some lysosomal proteins and accumulation of storage material. Both the central and peripheral retinas of these mice exhibited significant deterioration at 8.5 months (Damme et al. 2014). A subsequently generated Cln7 ko mouse displayed a more severe phenotype. Lysosomal dysfunction and defective autophagy resulted in neurodegeneration in the brain late during the disease, in neurological defects such as hind limb clapsing and myoclonus, and in an early-onset and rapidly progressing retinal degeneration (Brandenstein et al. 2016; Jankowiak et al. 2016).

1.3. Neurotrophic factors

Neurotrophic factors (NTFs) are proteins that promote the survival of specific nerve cell types during development and under pathological conditions. For the retina, a number of NTFs has been identified that rescue retinal ganglion cells (RGCs) and/or photoreceptor cells in a variety of neurodegenerative retinal disorders. Examples of such neuroprotective proteins include progranulin, rod-derived cone viability factor, vascular endothelial growth factor, basic fibroblast growth factor, leukemia inhibitory factor, glial cell line-derived growth factor or ciliary neurotrophic factor (CNTF) (Kuse et al. 2017; Mei et al. 2016; Ait-Ali et al. 2015; Arjunan et al. 2018; Lipinski et al. 2011; Arranz-Romera et al. 2021; Valiente-Soriano et al. 2019; Byrne et al. 2016; Joly et al. 2008; Fischer and Leibinger 2012; Xie et al. 2015; Flachsbarth et al. 2018; Dulz et al. 2020).
CNTF is a member of the interleukin 6 (IL-6) family of cytokines and exerts strong neuroprotective effects on various nerve cell types (Richardson 1994; Wen et al. 2012; Adler et al. 1979; Varon et al. 1979). In the retina, CNTF is secreted by various cell types, in particular by Müller glia cells (Kirsch et al. 1997). The cytokine is probably the most studied neuroprotective factor in the retina, and has been shown to potently rescue photoreceptor cells and RGCs (Cayouette and Gravel 1997; Cayouette et al. 1998; Chong et al. 1999; Tao et

al. 2002; Rhee et al. 2013; Wilson and Di Polo 2012; Almasieh et al. 2012; Leaver et al. 2006; Hellstrom et al. 2011; Flachsbarth et al. 2014; Pernet et al. 2013). Glial cell line-derived neurotrophic factor (GDNF) is a member of the GDNF family of ligands which belongs to the transforming growth factor-β (TGF-β) superfamily (Lin et al. 1993). Similar to CNTF, GDNF has been shown to promote survival of both, photoreceptors and ganglion cells (Frasson et al. 1999; Ohnaka et al. 2012; Koeberle and Ball 2002; Flachsbarth et al. 2018; Dulz et al. 2020). NTFs are unable to cross the blood-brain or blood-retina barrier and usually have a short half-life (Kolomeyer and Zarbin 2014; LaVail et al. 1992; Kurokawa et al. 1999; Vidal-Sanz et al. 2001; Takahata et al. 2003; Ejstrup et al. 2010; LaVail et al. 1998). Efficient neuroprotection therefore requires a direct and continuous application of NTFs to the diseased brain or retina. Methodologies to achieve these aims include gene therapy, transplantations of cell genetically modified to overexpress NTFs, or implantations of NTF-loaded slow-release devices (Birch et al. 2016; Birch et al. 2013; Bush et al. 2004; Kauper et al. 2012; Sieving et al. 2006; Zhang et al. 2011). In previous studies, our group has explored the efficacy of a cell-based neuroprotective approach to attenuate retinal degeneration in animal models of different neurodegenerative retinal disorders. To this aim, we established clonally derived neural stem cell (NSC) lines with a stable overexpression of CNTF or GDNF. Intravitreal transplantations of NSC lines overexpressing CNTF resulted in robust protection of photoreceptor cells in the phosphodiesterase 6B *(Pde6B)* mutations *Pde6b*^{rd1} and *Pde6b*^{rd10} mouse models of retinitis pigmentosa (RP) (Jung et al. 2013), the *CLN6*^{nclf} mouse model of CLN6 disease (Jankowiak et al. 2015) and in a marked protection of RGCs in an optic nerve crush model (Flachsbarth et al. 2014). Promotion of RGCs survival was also observed with the GDNF overexpressing cell clone. Of note, the combined administration of several NTFs showed synergistic effects in rescuing photoreceptor cells (Cuenca et al. 2014; Kolomeyer and Zarbin 2014). In line with these findings, we found a pronounced synergistic and long-lasting rescue of axotomized RGCs when the CNTF and the GDNF overexpressing cell lines were co-transplanted into the optic nerve crush model (Flachsbarth et al. 2018; Dulz et al. 2020). Here, we argued that a co-administration of both NTFs might exert a similar cooperative or possibly synergistic rescue effect on

photoreceptor cells in the *Cln7* ko mouse model. We therefore analyzed photoreceptor survival and retina function in animals treated separately with either CNTF or GDNF or simultaneously with both neuroprotective factors.

2. Material and Methods

2.1 Animals

Cln7 ko mice (Brandenstein et al. 2016) were housed in a pathogen-free animal facility at the University Medical Center Hamburg-Eppendorf in a 12 hours light/dark cycle and ad libitum access to food and water. Deoxyribonucleic acid (DNA) from tail was amplified by polymerase chain reaction (PCR) to identify the genotype of the offspring as indicated (Brandenstein et al. 2016). The local animal protection authority gave its approval to all animal experiments (acceptance no. 110/2019; ORG 842).

2.2 Lentiviral modification of neural stem cells

Clonal neural stem cell (NSC) lines stably expressing CNTF (CNTF-NSCs) or GDNF (GDNF-NSCs) together with a fluorescent reporter protein, and NSC lines expressing a reporter protein only for control experiments (control-NSCs) were generated as previously described (Flachsbarth et al. 2014; Flachsbarth et al. 2018; Dulz et al. 2020). Clonally derived NSC lines with high levels of NTF expression were established by repeated transductions, each followed by clonal expansion of the modified cells with the strongest levels of reporter protein production and thus with the highest NTF expression level (Jung et al. 2013). Using this strategy, the lab established a GDNF- and CNTF-expressing clonal NSC line that protected RGCs from axotomy-induced cell death with a similar efficacy.

2.3 Neural stem cell transplantation

NSCs were intravitreally injected into 14 days old mice. After removing 2µl of vitreous fluid with a micropipette attached to a syringe, 8×10^5 cells of either

the CNTF-NSC, GDNF-NSC or control-NSC line, or 8 × 10^5 cells of a 1:1 mixture of CNTF-NSCs and GDNF-NSCs were slowly injected into the vitreous cavity under visual control as described in detail elsewhere (Flachsbarth et al. 2014; Flachsbarth et al. 2018; Dulz et al. 2020).

2.4 Analyses of grafted neural stem cells

3.5 months after intravitreal cell injections, differentiation and transgene expression by the grafted NSCs were analyzed. Animals were sacrificed, and eyes were fixed for one hour in 4% paraformaldehyde (PA). To analyze the expression of both growth factors, lenses with attached NSCs were removed and stained with goat anti-GDNF and rabbit anti-CNTF antibodies. Neural differentiation of NSCs was analyzed using rabbit anti-glial fibrillary acidic protein (GFAP; Dako Cytomation GmbH, Hamburg, Germany; Z0334; 1:500) and mouse anti-β-tubulin III (Sigma-Aldrich; T8660; 1:1000) antibodies. Secondary antibodies conjugated to Cy3 or Cy5 (Jackson ImmunoResearch Inc.) were used to detect primary antibodies. Immunolabeled NSCs were analyzed with an Olympus FV 1000 confocal microscope (Olympus, Hamburg, Germany).

2.5 Immunohistochemistry

Cln7 ko mice were sacrificed at postnatal day (P) 56, 112 or 168. After enucleating the eyes, the temporal cornea was removed and the extraocular tissue was trimmed away carefully. Eyes were fixed in 4% PA in phosphate buffered saline (PBS; pH 7.4) overnight at room temperature. After fixation, eyes were dehydrated overnight at room temperature in ascending concentrations of sucrose (7.5%, 15% and 30%). The eyeballs were immersed in Tissue-Tek (Sakura Finetek, Zouterwoude, The Netherlands) and snap frozen in liquid nitrogen in a defined orientation to enable later identification of the nasal and temporal retinal periphery.

Eyes were serially cut at a thickness of 25µm with a cryostat (LEICA CM 1950, Leica Biosystems Nussloch GmbH, Germany) and stored in PBS before being blocked in PBS (pH 7.4) containing 0.1% bovine serum albumin (BSA) and 0.3%

Triton X-100 (both from Sigma-Aldrich Corp., St. Louis, MO, USA). Sections were incubated with biotinylated peanut agglutinin (PNA) for 2 days, followed by overnight incubation with Cy3-conjugated streptavidin. Incubation of sections with primary antibodies (see Table 1) was undertaken overnight at room temperature and 4 °C, followed by extensive washing with PBS and incubation with secondary antibodies. Before mounting of sections, cell nuclei were stained for 10 minutes with 4', 6-diamidino-2-phenylindole (DAPI; Sigma-Aldrich).

Table 1: Primary and secondary antibodies

Antigen	Dilution	Company/Reference	Catalog Number
PNA	1:5,000	Vector Laboratories, Burlingame, CA, USA	n.a.
cathepsin D (CTSD)	1:2,000	Santa Cruz Biotechnology, Inc.	Sc-6486
cathepsin X/Z/P (CTSZ)	1:100	R&D Systems GmbH	AF1033
cluster of differentiation 68 (CD68)	1:1,000	Bio Rad Laboratories, Kidlington, UK	MCA1957
glial fibrillary acidic protein (GFAP)	1:500	Dako Cytomation GmbH, Hamburg, Germany	Z0334
ionized calcium-binding adapter molecule 1 (IBA1)	1:2,000	Wako Chemicals GmbH, Neuss, Germany	O19-19741
lysosomal-associated membrane protein 1 (LAMP1)	1:2,000	Santa Cruz Biotechnology, Inc.	Sc-19992
lysosomal-associated membrane protein 2 (LAMP2)	1:200	Developmental Studies Hybridoma Bank, lowa City, IA, USA	Clone ABL93
protein kinase C alpha (PKCα)	1:500	Santa Cruz Biotechnology, Inc.	Sc-208
recoverin	1:3,000	Milllipore, Temecula, CA, USA	AB5585

sphingolipid activating proteins D (saposin D)	1:2,000	Konrad Sandhoff, Bonn, Germany (Klein et al. 1994)	n.a.
secretagogin (SCGN)	1:2,000	BioVendor Research and Diagnostic Products	RD184120100
sequestosome 1/p62 (SQSTM1/p62)	1:1,000	Enzo Life Sciences GmbH, Lörrach, Germany	BML-PW9860
subunit c of mitochondrial ATP synthase (SCMAS)	1:1,000	Abcam, Cambridge, UK	Ab181243
Cy3 anti-sheep	1:200	Jackson ImmunoResearch Laboratories, Inc	133179
Cy3 anti-strep (Cy3-conjugated streptavidin)	1:500	Jackson ImmunoResearch Laboratories, Inc	123835
Cy3 anti-goat	1:200	Jackson ImmunoResearch Laboratories, Inc	134527
Cy3 anti-rat	1:200	Jackson ImmunoResearch Laboratories, Inc	140333
Cy3 anti-rabbit	1:200	Jackson ImmunoResearch Laboratories, Inc	144186

n.a., not applicable

2.6 Analyses of retinal thinning and retinal nerve cell numbers

An AxioObserverZ.1 microscope equipped with an ApoTome.2 (Zeiss, Oberkochen, Germany) and ZEN2.3 software was used to capture images of entire central retinal sections from the nasal to the temporal margin.

The number of PNA-positive cone photoreceptor cells, PKCα-positive rod bipolar cells, and SCGN-positive cone bipolar cells provided the cells had a clearly visible nucleus was enumerated using Fiji Image J 1.51s software (Rasband, W.S., U.S. National Institutes of Health, Bethesda, MD, USA). Cells were counted in three defined areas located at positions corresponding to 25%, 50%, and 75% of the distance between the retina periphery and the optic disc

in both the temporal and nasal retina, each area with a width of 250µm. The density of PKCα-positive rod bipolar cells and SCGN-positive cone bipolar cells with a clearly discernible nucleus was additionally determined at the utmost edge of the temporal and nasal retinal periphery in an area spanning 250µm.
Ionized calcium-binding adapter molecule 1 (IBA1)-positive microglia cells were counted in entire central retina sections in the inner (from the inner nuclear layer (INL) to the vitreoretinal interface) and outer retina (from the outer plexiform layer (OPL) to the photoreceptor outer segments), whereas cluster of differentiation 68 (CD68)-positive microglia cells were enumerated exclusively in the outer retina.
Rows of DAPI-positive photoreceptor nuclei were counted in central retinal sections at nine equidistant positions between the optic nerve head (ONH) and the peripheral margin of both the nasal and temporal retina. The three most peripheral positions were defined as “peripheral retina”, while the three most central positions were defined as “central retina”.

2.7 Electroretinogram recordings

Electroretinograms (ERGs) were recorded from the surface of mice's corneas. In brief, animals were anesthetized subcutaneously with Ketanest S (PFIZER PHARMA PFE GmbH, Berlin, Germany) and Xylasin (Wirtschaftsgenossenschaft Deutscher Tieraerzte eG, Gargsen, Germany) after dark adaption (DA) for a minimum of 12 hours. An electric heating blanket was used to keep the body temperature at 38 °C. Neosynephrin-POS 5% (Arzneimittel GmbH, Saarbrücken, Germany) and Mydriaticum Stulln (Pharma Stulln GmbH, Stulln, Germany) were used to dilate pupils. One drop of Methocel 2% (OmniVision GmbH, Puchheim, Germany) was used to prevent corneal dehydration and to optimize electrical contact between the custom-made contact lens electrode and the cornea. Reference platinum needles were inserted subcutaneously in the nape of the neck, while the ground electrode was inserted subcutaneously in the posterior region of the back. A stimulus intensity of 9.49 cd s m^2 was delivered to dark adapted and dilated eyes with a Ganzfeld Q450 (Roland Consult Stasche & Finger GmbH, Brandenburg/Havel, Germany) to determine the scotopic response. The amplitude of the scotopic

a-wave was measured from the prestimulus baseline to the a-wave trough. The amplitude of the scotopic b-wave was determined from the trough of the a-wave to the peak of the b-wave. In case the b-wave´s peak corresponded with the oscillatory potentials (OP), the b-wave amplitude was determined using the highest signal value following the OP. To assess the photopic responses, animals were light adapted for 5 minutes under a 25 cd m^2 light source. Subsequently, a strobe light with an intensity of 9.49 cd s m^2 was delivered to the dilated eyes using the Ganzfeld Q450. The photopic b-wave amplitude was determined from the trough of the a-wave to the highest value of the b-wave. Following ERG recordings, Corneregel (Dr. Mann Pharma GmbH, Berlin, Germany) was used to prevent dehydration of corneas.
Statistical analyses of data from the morphometric analyses or ERG recordings were performed using Prism 9 software (GraphPad Software, San Diego, CA, USA).

3. Results

3.1 Progressive loss of multiple retinal cell types in untreated *Cln7* knockout mice

Cln7 ko retinas display a significant progressive retinal thinning (Jankowiak et al. 2016), indicative for a loss of various retinal cell types in the mutant retina. To identify the retinal cell types affected by CLN7 deficiency and to assess the time course of their degeneration, we employed a panel of cell type-specific markers and determined the density of different cell types at different developmental ages.

3.1.1 Cone photoreceptor cells

To determine whether CLN7 deficiency affects cone photoreceptor cell survival, retinal sections were stained with the lectin peanut agglutinin (PNA) to specifically visualize cones (Fig. 1A).
PNA staining revealed a significantly reduced number of cones in *Cln7* ko

peripheral retinas at 2 months of age (Fig. 1Ac, 1Ad, 1Bb), with 10.3 ±0.7 cones/250µm retina length (mean ±SEM) in mutant retinas compared to 18.4 ±0.4 cones/250 µm in age-matched wild-type (wt) retinas ($p<0.001$; two-way analysis of variance (ANOVA)). The density of cones in entire *Cln7* ko retinas (Fig. 1Aa, 1Ab, 1Ba), in comparison, was similar to that of wt retinas (18.6 ±0.6 cones/250µm in mutants, 19.9 ±0.3 cones/250µm in wt).

In 4 and 6 months old animals, mutant entire retinas contained 16.6 ±0.2 and 15.2 ±0.4 cones/250µm respectively (Fig. 1Ae, 1Af, 1Ai, 1Aj, 1Ba), while wt retinas contained 20.6 ±0.3 and 20.2 ±0.2 cones/250µm respectively ($p<0.001$ for both comparisons). A marked loss of cones was observed in the peripheral retina of 4 and 6 months old mutants (Fig. 1Ag, 1Ah, 1Ak, 1Al). While the density of cones in *Cln7* ko retinas was reduced to 5.2 ±0.8 and 2.1 ±0.3 cones/250µm retina length at 4 and 6 months of age respectively (Fig. 1Bb), wt peripheral retinas contained 15.7 ±0.9 and 13.7 ±0.6 cones/250 µm retina length, respectively ($p<0.001$ for both comparisons).

Quantitative analyses revealed that about 24.5% of the cones were lost in the entire mutant retina at 6-month-old (Fig. 1Ba), with 15.2 ±0.4 cones/250µm in *Cln7* ko retinas as opposed to 20.2 ±0.2 cones/250µm in wt retinas ($p<0.001$; two-way ANOVA followed by Tukey's multiple comparison test; Fig. 1Ba).

(page breaks)

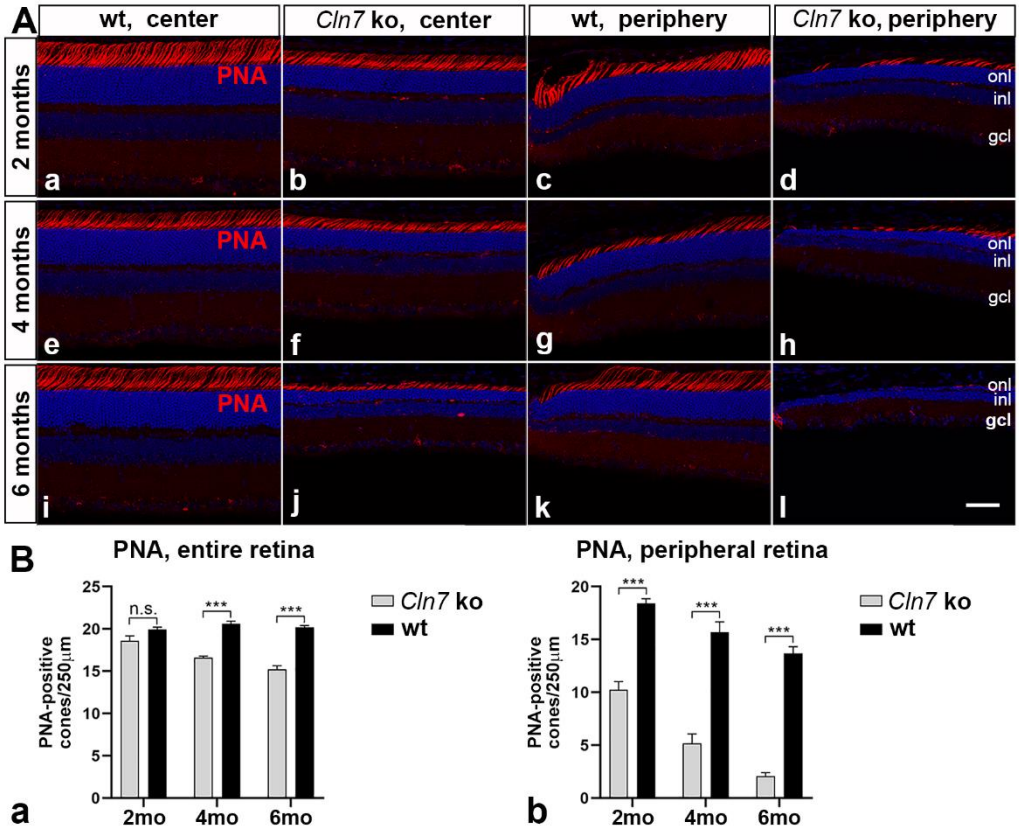

Figure 1: Degeneration of cone photoreceptor cells.
(A) The density of PNA-positive cone photoreceptor cells in the peripheral retina was significantly reduced in 2 months old *Cln7* ko mice (Ad) when compared to age-matched wt mice (Ac), while the density of cone photoreceptor cells in the central retina of *Cln7* ko mice (Ab) was similar to that of age-matched wt retinas (Aa). Note the reduced length of inner and outer segments of cones in the mutant at this age (Ab, Ad). In 4 and 6 months old mutant retinas, a pronounced loss of cones was evident in both the entire and the peripheral retina (Af, Ah, Aj, Al). (B) Quantitative analyses of entire mutant (open bars in Ba) and wt (filled bars in Ba) retinas revealed no difference in the density of cones in 2 months old animals, but a significantly reduced cone density in 4 and 6 months old *Cln7* ko mice retinas (Ba). The loss of cones at these ages was markedly more pronounced in the periphery of mutant retinas (Bb). Each bar represents the mean value (±SEM) of at least 6 animals. *, p<0.05; **, p<0.01; ***, p<0.001, two-way ANOVA followed by Tukey's multiple comparisons test. gcl, ganglion cell layer; inl, inner nuclear layer; ko, knock-out; n.s., not significant; onl, outer nuclear layer; wt, wild-type. Scale bar in (Al) for (Aa-Al): 50µm.

Notably, there was no statistically significant difference in the number of PNA-positive cone photoreceptor cells between 4 months old (16.6 ±0.2 cones/250µm) and 6 months old (15.2 ±0.4 cones/250µm) *Cln7* ko mice in the entire retina, indicating a relatively slowly progressing degeneration of this photoreceptor type.

3.1.2 Rod and cone bipolar cell

To determine if CLN7 deficiency affects rod and cone bipolar cells in addition to cone photoreceptor cells, retinal sections were stained with antibodies to PKCα and SCGN, respectively (Fig. 3A and Fig. 2A, respectively).

The density of both nerve cell types in entire *Cln7* ko retinas was significantly decreased at 2 months of age (Fig. 2Aa, 2Ab, 3Aa, 3Ab), with 27.1 ±0.5 rod bipolar cells/250µm retina length (mean ±SEM) and 20.9 ±0.7 cone bipolar cells/250µm in mutant retinas compared to 34.0 ±0.3 rod bipolar cells/250µm and 28.4 ±0.8 cone bipolar cells/250µm in wt retinas ($p<0.001$ for both comparisons; Fig. 2B). Peripheral mutant retinas, in comparison, contained 22.7 ±0.6 rod bipolar cells/250µm and 12.7 ±0.7 cone bipolar cells/250µm compared to 27.8 ±0.4 rod bipolar cells/250µm and 18.9 ±0.5 cone bipolar cells/250µm in wt retinas ($p<0.001$ for both comparisons; Fig. 2B).

At 4 months of age, rod and cone bipolar cells numbers in entire mutant retinas were 21.7 ±0.2/250µm and 19.4 ±0.4/250µm respectively, compared to 33.5 ±0.3/250µm and 29.3 ±0.3/250µm respectively in wt retinas ($p<0.001$ for both comparisons; Fig. 2B). Peripheral retina regions contained 16.6 ±0.4 rod bipolar cells/250µm and 7.8 ±0.4 cone bipolar cells/250µm in *Cln7* ko retinas and 23.1 ±0.4 rod bipolar cells/250µm and 16.8 ±0.8 cone bipolar cells/250µm in wt retinas ($p<0.001$ for both comparisons; Fig. 2B).

At 6 months of age, rod and cone bipolar cells numbers in mutant entire retinas accounted for 40.6% and 58.3% respectively of the rod and cone bipolar cell numbers observed in age-matched wt retinas. In peripheral retinas, the density of rod bipolar cells in mutants was markedly reduced, accounting to only 16.8% of the rod bipolar cell density found in age-matched wt mice. Loss of cone bipolar cells, in comparison, was more moderate with 53.4% of the value observed in wt (Fig. 2B).

(page breaks)

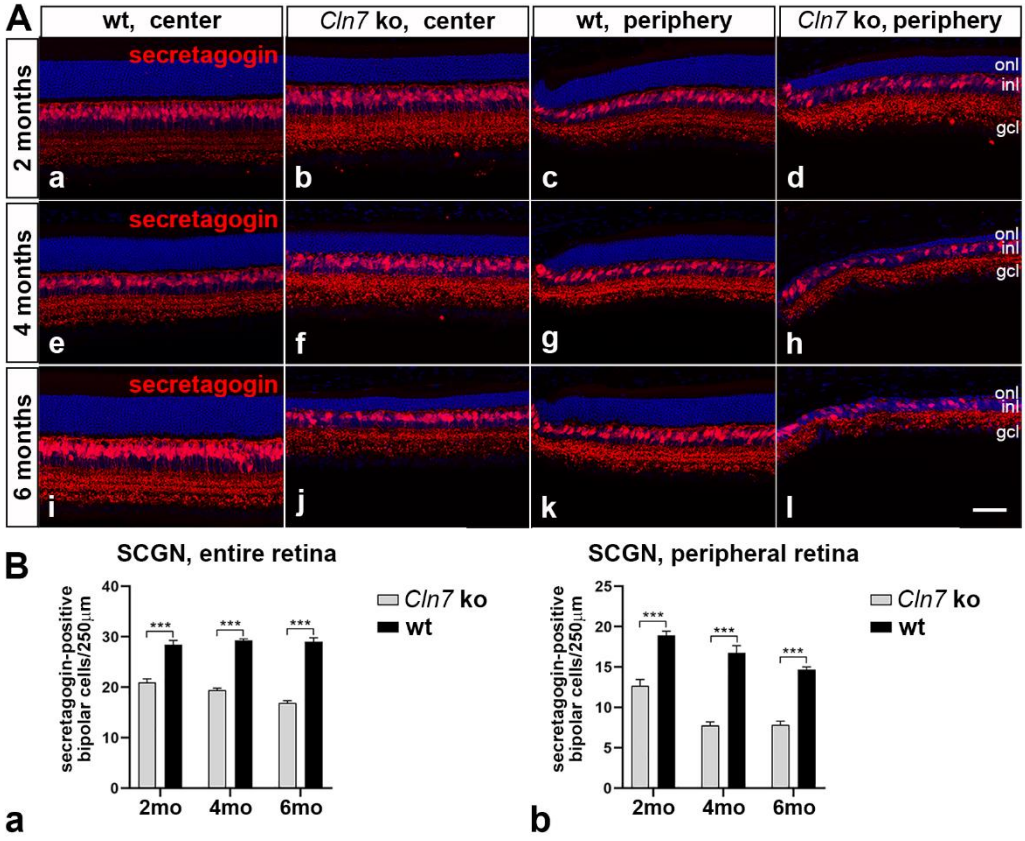

Figure 2: Degeneration of cone bipolar cells.

(A) A significant loss of SCGN-positive cone bipolar cells was apparent in both the centre and periphery of the retina of 2, 4 and 6 months old *Cln7* ko retinas (Ab, Af, Aj, Ad, Ah, Al) when compared to age-matched wt mice (Aa, Ae, Ai, Ac, Ag, Ak). (B) Quantitative analyses of mutant (open bars in Ba and Bb) and wt retinas (filled bars in Ba and Bb) revealed a significant loss of cone bipolar cells in the entire (Ba) and particularly in the peripheral retina (Bb). Each bar represents the mean value (±SEM) of at least 6 animals. *, $p<0.05$; **, $p<0.01$; ***, $p<0.001$, two-way ANOVA followed by Tukey's multiple comparison test. gcl, ganglion cell layer; inl, inner nuclear layer; ko, knock-out; n.s., not significant; onl, outer nuclear layer; wt, wild-type. Scale bar in (Al) for (Aa-Al): 50µm.

(page breaks)

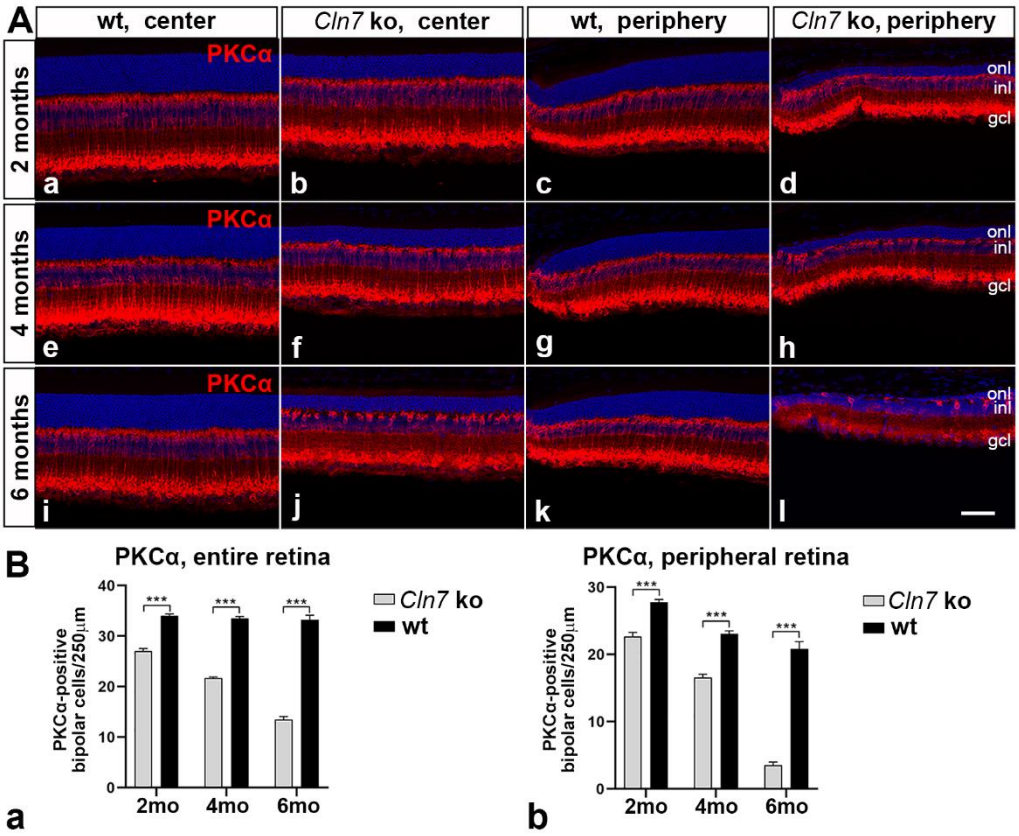

Figure 3: Degeneration of rod bipolar cells.

(A) A significant loss of PKCα-positive rod bipolar cells was evident in both the central and peripheral retina regions of 2, 4 and 6 months old *Cln7* ko mice (Ab, Af, Aj, Ad, Ah, Al) when compared to age-matched wt mice (Aa, Ae, Ai, Ac, Ag, Ak). (B) Quantitative analyses of wt (filled bars in Ba and Bb) and mutant (open bars in Ba and Bb) retinas revealed a significant loss of rod bipolar cells in the entire (Ba) and peripheral retina (Bb) which was particularly pronounced in 6 months old animals (Bb). Each bar represents the mean value (±SEM) of at least 6 animals. *, p<0.05; **, p<0.01; ***, p<0.001, two-way ANOVA followed by Tukey's multiple comparison test. gcl, ganglion cell layer; inl, inner nuclear layer; ko, knock-out; n.s., not significant; onl, outer nuclear layer; wt, wild-type. Scale bar in (Al) for (Aa-Al): 50µm.

3.1.3 Electroretinogram recordings in untreated *Cln7* knockout mice

Electroretinography (ERG) was used to evaluate the retinal function of *Cln7* ko mice. The amplitudes of the scotopic a-wave in *Cln7* ko mice at 2, 4, and 6 months of age (216.2 ±2.8 µV, 113.1 ±9.0 µV and 62.9 ±7.6 µV (mean ±SEM), respectively) were significantly lower than in wild-type mice (541.4 ±16.9 µV,

547.6 ±23.8 µV and 436.8 ±14.5 µV (mean ±SEM), respectively). In addition, amplitudes of the scotopic b-wave were substantially decreased at 2 and 4 months of age, with 668.8 ±31.8 µV and 379.8 ±18.7 µV in *Cln7* ko mice compared to 924.3 ±25.4 µV and 890.5 ±27.3 µV in wild-type mice. Scotopic b-wave amplitudes further decreased to about 24% of those of wild-type mice in 6 months old mutants. Photopic a-waves in mice are negligible (Peachey et al. 1993). Cone-driven photopic b-wave amplitudes were similar in 2 months old *Cln7* ko mice (184.2 ±7.5 µV) and age-matched wild-type mice (185.3 ±14.7 µV). However, there is a considerable decrease in photopic b-wave amplitudes at 4 and 6 months of age with 125.6 ±5.6 µV and 81.7 ±7.0 µV respectively compared to 193.3 ±5.1 µV and 191.6 ±12.5 µV respectively in wild-type mice. In summary, scotopic a-wave and b-wave amplitudes in *Cln7* ko mice were significantly lower than in wild-type mice at 2, 4, and 6 months of age (Fig. 4A and Fig. 4B). Data are consistent with the morphological findings demonstrating a progressive degeneration of rod photoreceptor cells and rod bipolar cells.

Normal photopic ERG b-wave amplitudes indicated the existence of functionally intact cone-to-inner retina signaling in 2 months old mutant mice. However, at 4 months of age, cone-driven signaling to the inner retina was considerably impaired in *Cln7* ko animals compared to wild-type mice. Retina function was more severely affected in 6 months old mutants.

(page breaks)

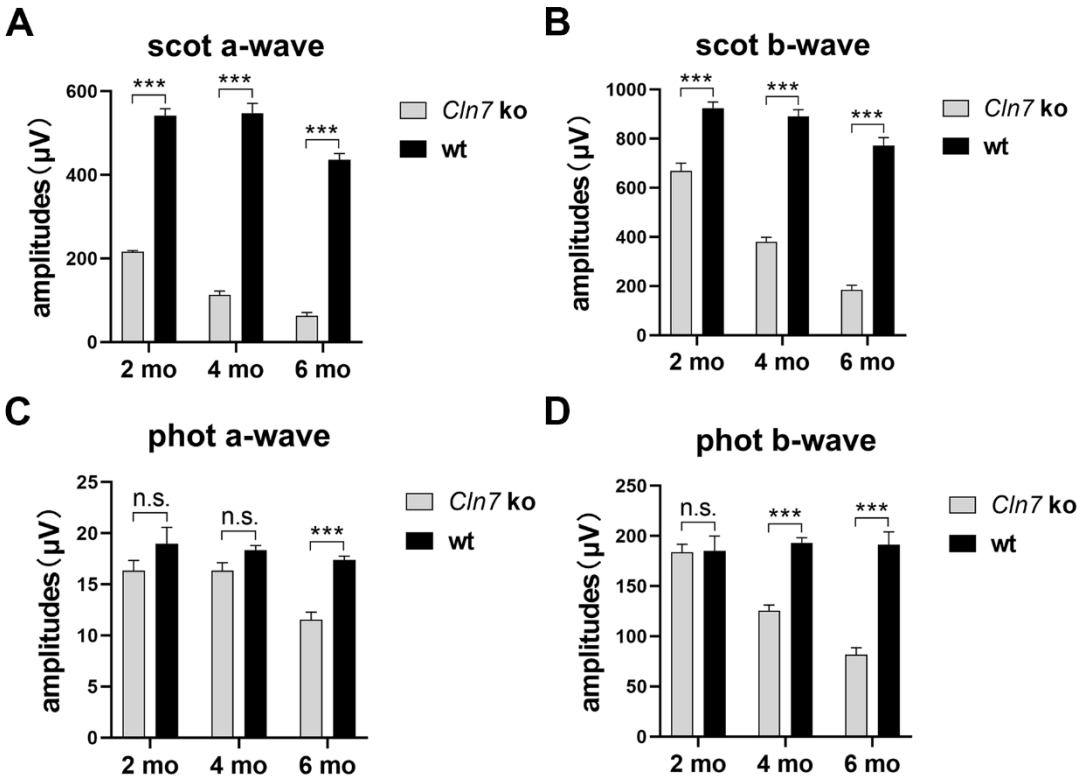

Figure 4 Electroretinogram recordings in wild-type and *Cln7* ko mice at 2, 4 and 6 months of age.

Bars represent the amplitudes of photopic a- and b-waves and scotopic a- and b-waves in wt mice (filled bar) *Cln7* ko mice (open bar) to a light stimulus of 10 log cd s m−2. Each bar represents the mean value (±SEM) of at least 6 animals. *, p<0.05; **, p<0.01; ***, p<0.001, two-way ANOVA followed by Tukey's multiple comparison test. n.s., not significant.

3.2 Neural stem cell-based neuroprotection for the treatment of retinal degeneration in *Cln7* knockout mice

3.2.1 Differentiation and transgene expression in grafted neural stem cells *in vivo*

To analyze the therapeutic impact of a cell-based neuroprotective strategy aimed at attenuating retinal degeneration in *Cln7* ko mice, we grafted NSC lines with a stable expression of neurotrophic factors into the vitreous cavity of 14 days old *Cln7* ko mice. Intravitreal transplantations of a NSC line expressing a

fluorescent reporter protein but no neurotrophic factor into the contralateral eyes served as a control. Survival, intraocular localization, neural differentiation and transgene expression of the grafted cells were analyzed in 4 months old animals, 3.5 months after the transplantation. Grafted GDNF-NSCs, CNTF-NSCs and control-NSCs in host eyes were identified by the expression of the reporter genes.

All NSC lines survived the 3.5 months post-transplantation interval and were preferentially located on the posterior surface of the lenses (Fig. 5 and Fig 6) and the anterior surface of the retinas (not shown). Control-NSCs (Fig. 5e) and CNTF-NSCs (not shown) differentiated preferentially into GFAP-positive astrocytes (Fig. 5e) and only rarely into β-tubulin III-positive neurons (Fig. 5f). However, when GDNF- and CNTF-NSCs were grafted as a 1:1 mixture, a significant proportion of cells differentiated into β-tubulin III-positive neurons (Fig. 1c)

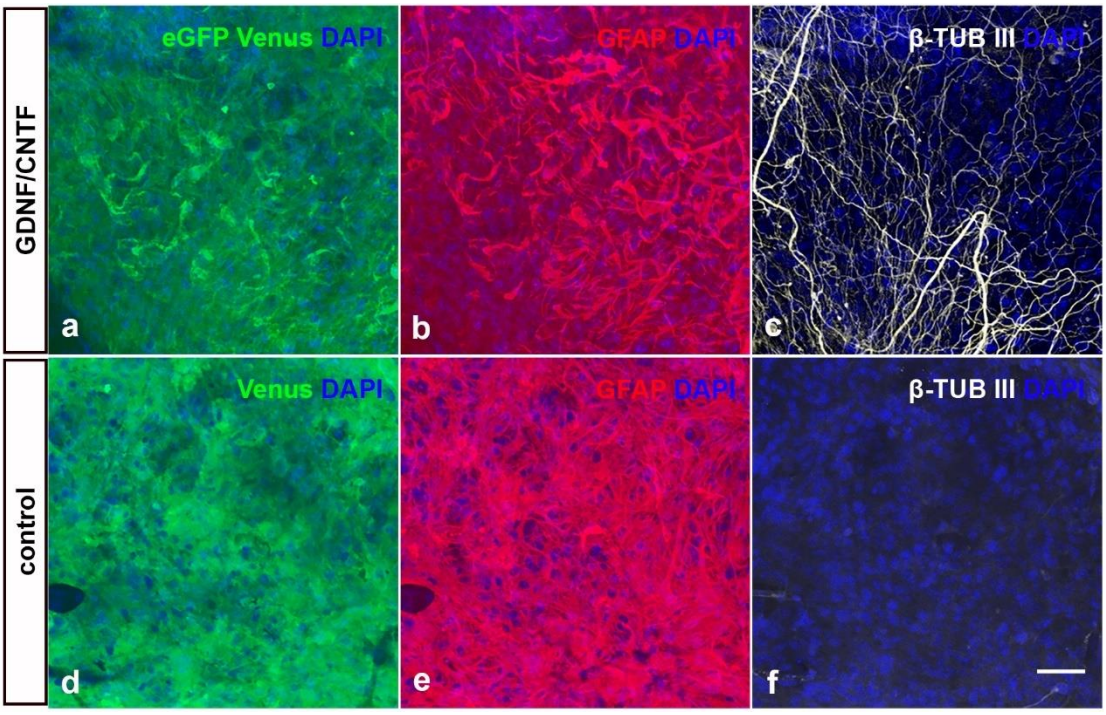

Figure 5: Differentiation of transplanted neural stem cells *in vivo*.
GDNF/CNTF-NSCs and control-NSCs were found on the posterior surface of the lenses. The grafted cell lines expressed the fluorescent reporter proteins (a, d) and were preferentially differentiated into GFAP-positive astrocytes (b, e). When CNTF-NSCs and GDNF-NSCs were grafted as a 1:1 mixture, a significant fraction of cells differentiated into neurons with positive expression of β-tubulin III (c). Scale bar in (f) for (a-f): 50µm

Furthermore, the grafted GDNF/CNTF-NSCs expressed the neurotrophic

factors and the reporter proteins eGFP or Venus over the entire post-transplantation period (Fig. 6a-c). Control-NSCs, in comparison, expressed the reporter gene only but no detectable amount of GDNF or CNTF (Fig. 6d-f).

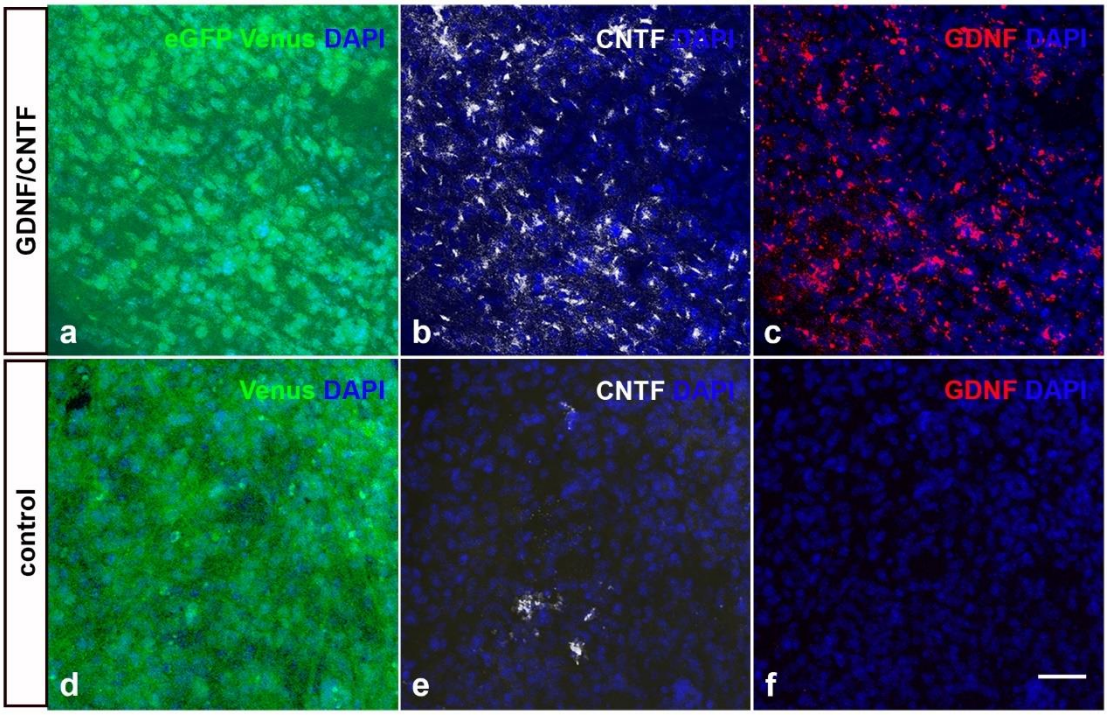

Figure 6: Expression of transgenes in grafted neural stem cells *in vivo*.
GDNF/CNTF-NSCs (a-c) and control-NSCs (d-f) were attached on the posterior side of the lens. GDNF/CNTF-NSCs expressed the reporter genes (a) and CNTF (b) or GDNF (c), while control-NSCs expressed the reporter gene only (d-f). Scale bar in (f) for (a-f): 50µm.

3.2.2 Impact of the neuroprotective treatment on expression levels of lysosomal proteins

To analyze whether the NSCs-based neuroprotective treatments affected the dysregulated expression of lysosomal proteins in *Cln7* ko retinas, we conducted immunostainings with antibodies against LAMP1 (Fig. 7a-h), LAMP2 (Fig. 7i-p), CTSD (Fig. 8a-h) and CTSZ (Fig. 8i-p). LAMP1, LAMP2, CSTD and CTSZ expression levels were significantly increased in 4-month-old *Cln7* ko mouse retinas when compared to 2-month-old *Cln7* ko retinas. At each age, however, intensity and distribution of all these lysosomal proteins were similar in retinas treated with either control-NSCs (Fig .7a, 7e, 7i, 7m, 8a, 8e, 8i, 8m), CNTF-

NSCs (Fig. 7d, 7h, 7l, 7p, 8d, 8h, 8l, 8p), GDNF/CNTF-NSCs (Fig. 7c, 7g, 7k, 7o, 8c, 8g, 8k, 8o) and GDNF-NSCs (Fig. 7b, 7f, 7j, 7n, 8b, 8f, 8j, 8n). The sustained intraocular administration of CNTF or GDNF or both neurotrophic factors had no beneficial effect on lysosomal homeostasis when compared to retinas treated with control-NSCs.

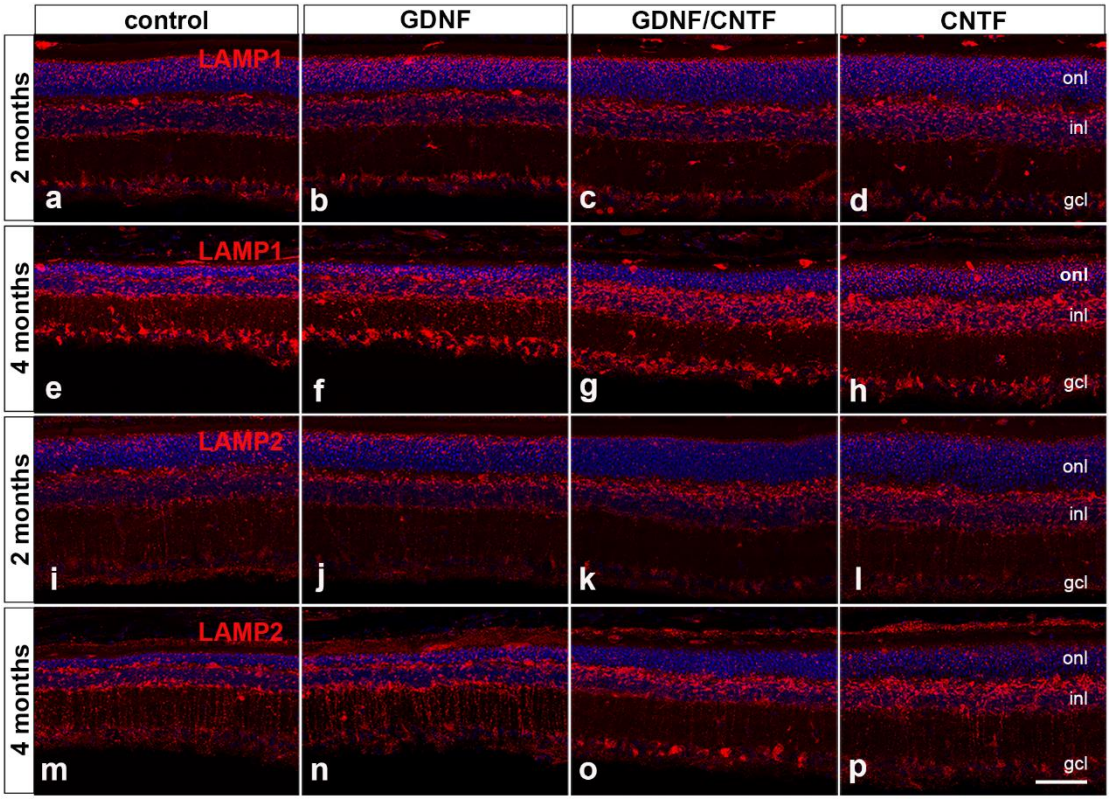

Figure 7: No effect of the neuroprotective treatment on expression levels of the lysosomal proteins LAMP1 and LAMP2.
Immunohistochemical analyses revealed elevated LAMP1 and LAMP2 expression levels in 4 months old control and treated *Cln7* ko retinas when compared to 2 months old retinas. No differences in LAMP1 and LAMP2 expression levels were detectable between 2 or 4 months old control retinas (a, e, i, m) and age-matched retinas treated with either GDNF-NSCs (b, f, j, n), GDNF/CNTF-NSCs (c, g, k, o) or CNTF-NSCs (d, h, l, p). gcl, ganglion cell layer; inl, inner nuclear layer; onl, outer nuclear layer; Scale bar in (p) for (a-p): 50µm.

(page breaks)

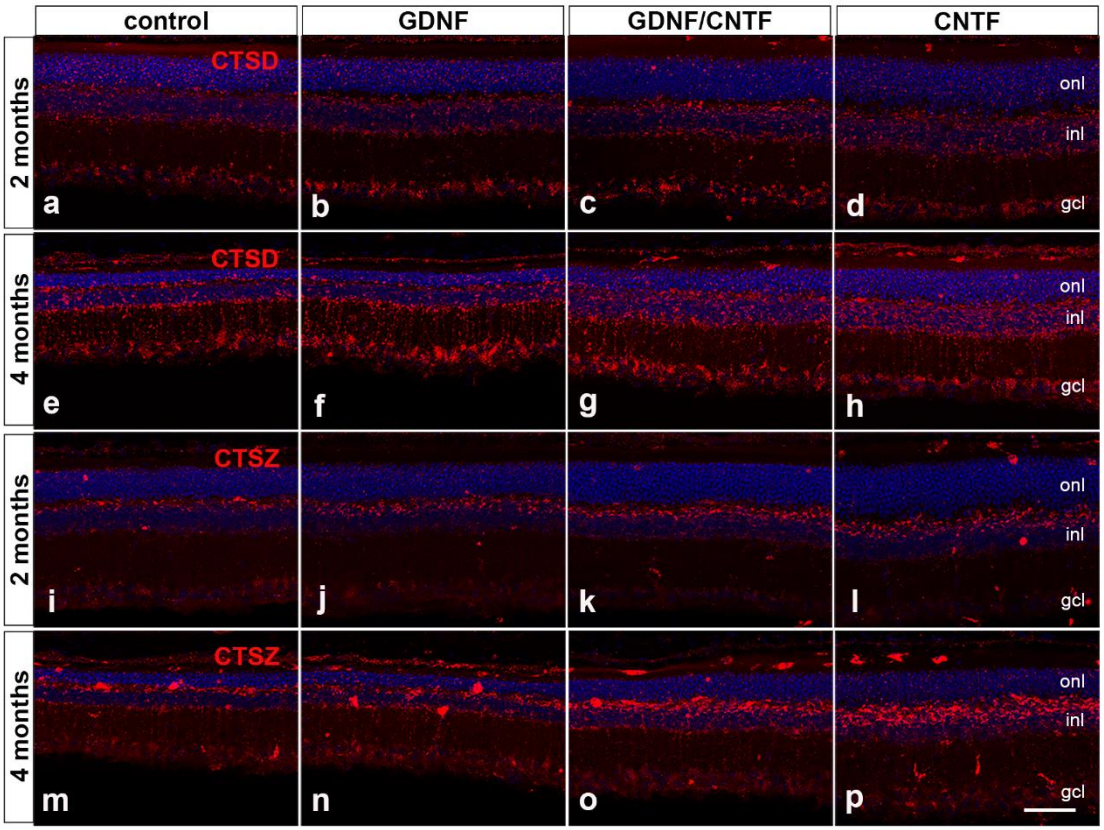

Figure 8: No effect of the neuroprotective treatment on expression levels of the lysosomal enzymes CTSD and CTSZ.
Immunohistochemical analyses revealed elevated CTSD and CTSZ expression levels in 4 months old control and treated *Cln7* ko retinas when compared to 2 months old retinas. No differences in CTSD and CTSZ expression levels were detectable between 2 or 4 months old control retinas (a, e, i, m) and age-matched retinas treated with either either GDNF-NSCs (b ,f, j, n), GDNF/CNTF-NSCs (c, g, k, o) or CNTF-NSCs (d, h, l, p). gcl, ganglion cell layer; inl, inner nuclear layer; onl, outer nuclear layer; Scale bar in (p) for (a-p): 50µm.

3.2.3 Impact of the neuroprotective treatment on the accumulation of storage material and the autophagy marker SQSTM1/p62

Immunohistochemistry with antibodies to SCMAS and saposin D was utilized to evaluate the accumulation of storage material in *Cln7* ko retinas (Fig. 9). SCMAS- and saposin D-immunoreactivity was more intense in 4 months old mutant retinas when compared to 2 months old animals, indicating progressive accumulation of storage material. Compared to mutant retinas treated with

control-NSCs (Fig. 9a, 9e, 9i, 9m), saposin D and SCMAS were detected in a similar distribution and at similar levels in retinas treated with GDNF-NSCs (Fig. 9b, 9f, 9j, 9n), GDNF/CNTF-NSCs (Fig. 9c, 9g, 9k, 9o) and CNTF-NSCs (Fig. 9d, 9h, 9l, 9p) at each age. Results indicate that the neurotrophic factors have no impact on the accumulation of lysosomal storage material.

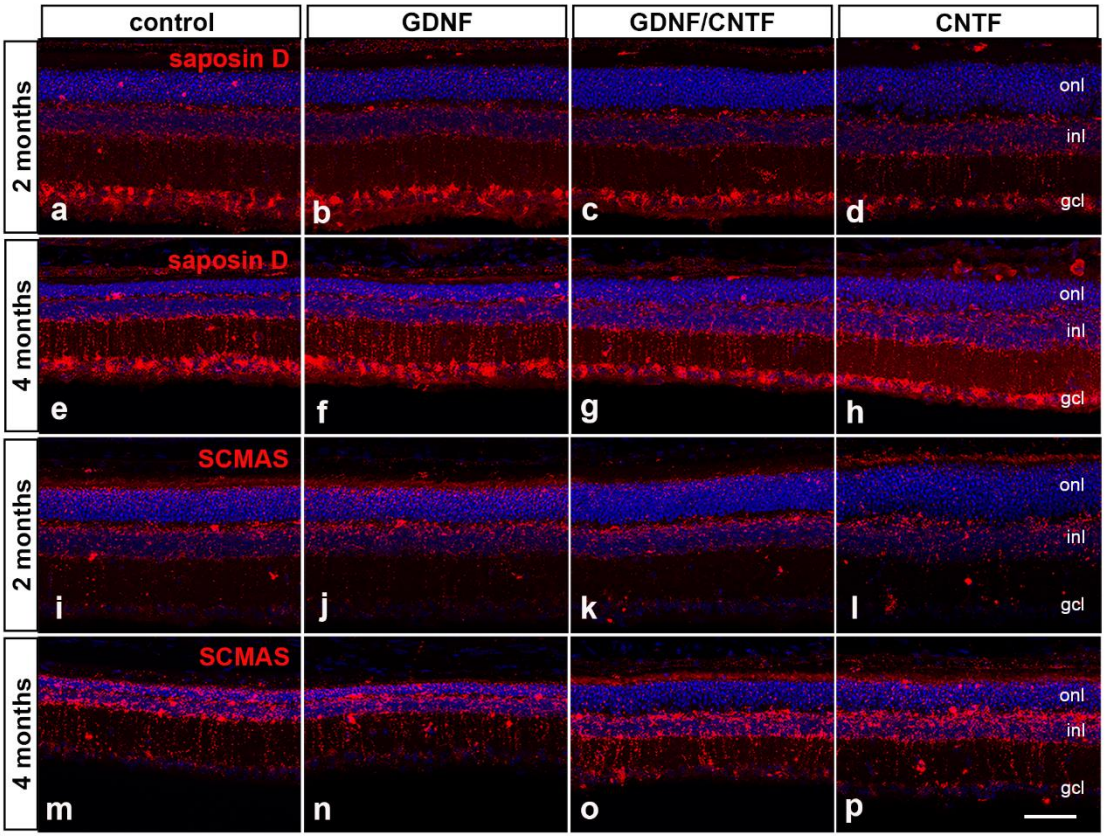

Figure 9: No effect of the neuroprotective treatment on the accumulation of storage material.

Saposin D (a-h) and SCMAS immunostainings (i-p) revealed an increase in the amount of storage material in *Cln7* ko retinas between the second (a-d; i-l) and fourth (e-h; m-p) postnatal months. At each age, there were no apparent differences in the intensity of the saposin D- or SCMAS-immunoreactivity in retinas with grafted control-NSCs (a, e, i, m) and grafted GDNF-NSCs (b, f, j, n), GDNF/CNTF-NSCs (e, g, k, o) or CNTF-NSCs (d, h, l, p). gcl, ganglion cell layer; inl, inner nuclear layer; onl, outer nuclear layer; Scale bar in (p) for (a-p): 50µm.

A decrease in SQSTM1/p62, a selective autophagy marker, indicates autophagy activation (Zhou et al. 2020) while accumulation of SQSTM1/p62 upon autophagy activation (e.g. by starvation) indicates autophagy impairment

(Klionsky et al. 2021). We used immunostaining with antibodies against SQSTM1/p62 to determine the autophagy state of *Cln7* ko retinas (Fig. 10). SQSTM1/p62-positive punctae were primarily restricted to the inner nuclear layer with a similar density in 2- (Fig. 10a-d) and 4-month-old *Cln7* ko retinas (Fig. 10e-h). The density and the intensity of the immunoreactive punctae was also similar between all retinas treated with the different clonal NSC lines (Fig. 10b-d and 10f-h).

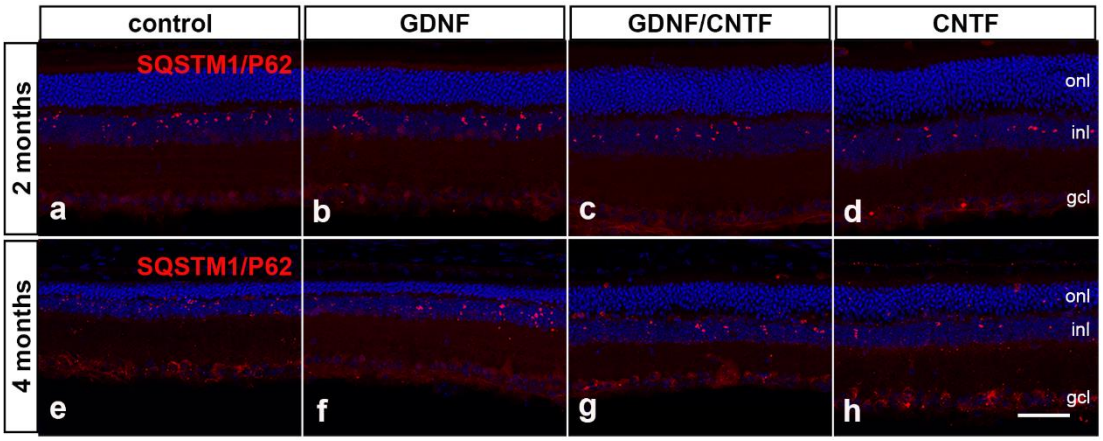

Figure 10: No effect of the neuroprotective treatment on the accumulation of the autophagy marker SQSTM1/p62.
The autophagy marker SQSTM1/p62 was preferentially found in the inner nuclear layer of 2 (a-d) and 4 (e-h) months old *Cln7* ko retinas, with no significant differences in the density of SQSTM1/p62-positive punctae between retinas with grafted control-NSCs (a,e) and grafted GDNF-NSCs (b,f), GDNF/CNTF-NSCs (c,g) or CNTF-NSCs (d,h). gcl, ganglion cell layer; inl, inner nuclear layer; onl, outer nuclear layer; Scale bar in (h) for (a-h): 50µm.

3.2.4 Impact of the neuroprotective treatment on neuroinflammation

Cln7 ko retina sections were stained with anti-GFAP (Fig. 12), anti-IBA1 (Fig. 11a-h), and anti-CD68 (Fig. 11i-p) antibodies to determine the effect of NSC therapy on reactive astrogliosis and reactive microgliosis. Results revealed a higher density of IBA1-positive cells (Fig. 11a-h), CD68-positive cells (Fig. 11i-p), and GFAP-positive cells (Fig. 12) in 4 months old retinas as compared to 2 months old retinas, in line with a previous study (Jankowiak et al. 2016).
Quantitative analyses revealed that the treatment with neurotrophic factors had no impact on the number of IBA1- (Fig. 11Ba) and CD68-positive microglial cells (Fig. 11Bb) when compared to control-NSCs treated retinas. In the CNTF-NSCs

group (Fig. 11Ba), the mean number of IBA1-positive microglia cells per 250µm retina length was 108.8 ±3.4 (mean ±SEM) and 143.3 ±5.0 in 2 and 4 months old animals respectively, whereas the mean number of IBA1-positive microglia cells per 250m retina length in control retinas was 103.5 ±5.0 and 142.9 ±5.3, respectively ($p > 0.05$; two-way ANOVA). In the GDNF-NSCs group (Fig. 11Ba), retinas contained 101.5 ±4.7 and 145.2 ±4.3 microglia cells/250µm at 2 and 4 month of age respectively, while control retinas contained 106.3 ±6.0 and 144.1 ±3.5 microglia cells/250µm, respectively ($p > 0.05$; two-way ANOVA). In the GDNF/CNTF-NSCs group (Fig. 11Ba), we found 107.1 ±6.3 and 142.2 ±4.6 microglia cells/250µm in 2 and 4 months old retinas respectively, compared to 102.5 ±6.8 and 137.4 ±6.2 microglia cells/250µm in the contralateral eyes, respectively ($p > 0.05$; two-way ANOVA; Fig. 11Aa-h, Ba).

Similar to the results obtained for IBA1-positive cells, we observed an overall increase in the density of CD68-positive with increasing age of the mutants (Fig. 11i-p). Also similar to the IBA1 results, there was no effect of the treatments on the density of CD68-positive microglia/macrophages at each age. In 2 months old animals, we found 65.8 ±6.5 cells/250µm retina length in CNTF-NSCs retinas and 44.7 ±7.6 cells in control retinas, 44.4 ±4.4 cells in GDNF-NSCs retinas and 58.4 ±15.5 cells in control retinas, and 82.7 ±13.8 cells in GDNF/CNTF-NSCs retinas and 69.7 ±10.1 cells in control retinas (Fig. 11Bb). The density values for CD68-positive cells in 4 months old mutants were 93.9 ±6.9 cells in CNTF-NSCs retinas and 99.7 ±8.3 cells in control retinas, 64.1 ±4.3 cells in GDNF-NSCs retinas and 73.1 ±7.7 cells in control retinas, and 97.9 ±5.4 cells in GDNF/CNTF NSCs retinas and 72.1 ±9.8 cells in control retinas (Fig. 11Bb; $p>0.05$ for all comparisons; two-way ANOVA).

(page breaks)

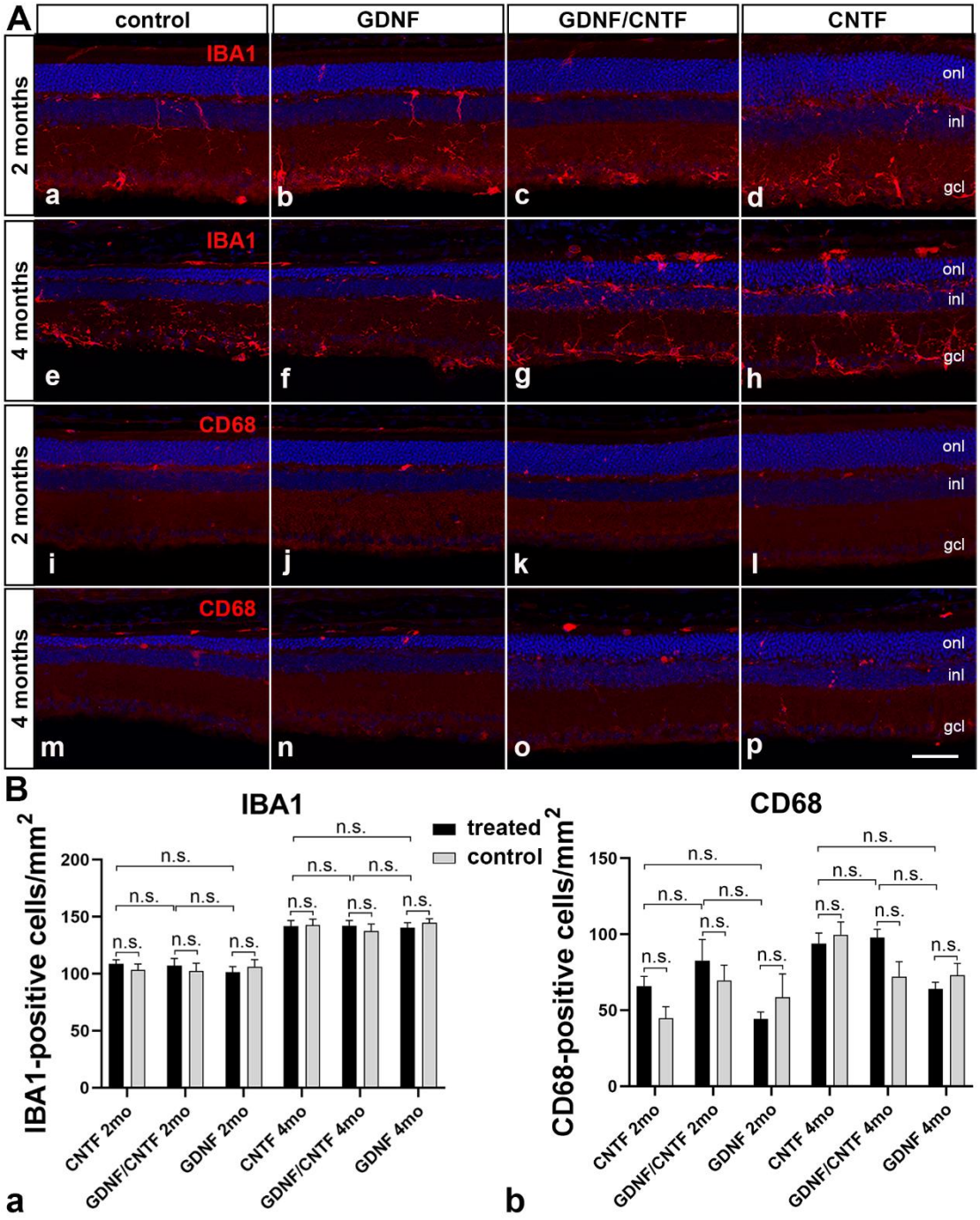

Figure 11: No effect of the neuroprotective treatment on reactive microgliosis.

(A) The density of IBA1- (a-h) and CD68–positive cells (I-p) were increased in 4 months old *Cln7* ko retinas (e-h; m-p) when compared to 2 months old animals (a-d; i-l). At each age, the density of microglial cells was similar in retinas with grafted control-NSCs (a, e, i, m) and grafted GDNF-NSCs (b, f, j, n), GDNF/CNTF-NSCs (c, g, k, o) or CNTF-NSCs (d, h, l, p). (B) Quantitative analyses of IBA1-positive microglial cells (Ba) and CD68-positive microglial cells (Bb) confirmed similar cell densities in control retinas (grey bars) and CNTF-, GDNF/CNTF- or GDNF-treated retinas (filled bars). Each bar represents the

mean value (±SEM) of 6 animals. Two-way ANOVA followed by Tukey's multiple comparison test. gcl, ganglion cell layer; inl, inner nuclear layer; onl, outer nuclear layer; n.s., not significant. Scale bar in (p) for (a-p): 50µm.

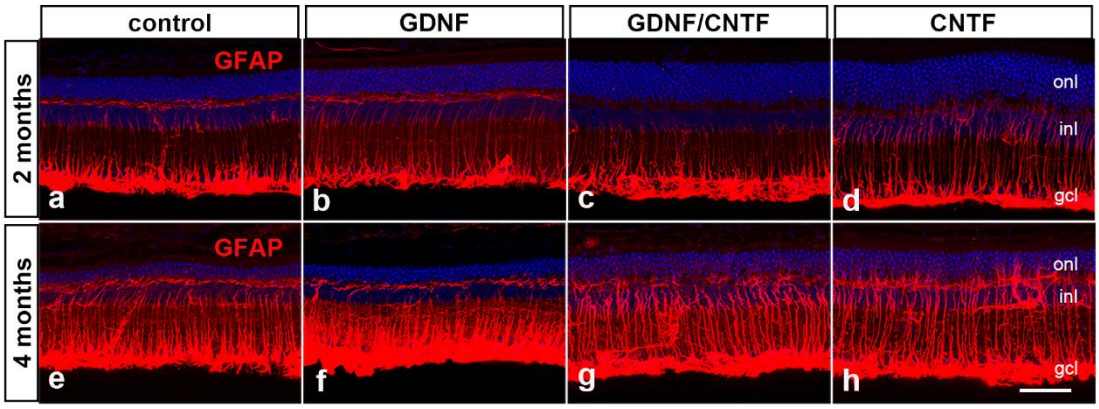

Figure 12: No effect of the neuroprotective treatment on reactive astrogliosis. Expression of GFAP in Müller cells and astrocytes was increased in 4 months old *Cln7* ko retinas (e-h) when compared to 2 months old animals (a-d). There were no differences in the intensity of the GFAP immunostaining between retinas with grafted control-NSCs (a, e) and retinas with grafted GDNF-NSCs (b, f), GDNF/CNTF-NSCs (c, g) or CNTF-NSCs (d, h). gcl, ganglion cell layer; inl, inner nuclear layer; onl, outer nuclear layer; Scale bar in (h) for (a-h): 50µm.

3.2.5 Impact of the neuroprotective treatment on the survival of various retinal nerve cell types

Given that rod photoreceptor cells constitute the vast majority of photoreceptor cells in the mouse retina, we determined the number of rows of photoreceptor nuclei to quantify the therapeutic impact of the neuroprotective treatment on this photoreceptor type.

At 2 and 4 months of age there was no significant difference in the number of rows of photoreceptor nuclei between retinas treated with GDNF-NSCs (4.9 ±0.2 rows and 2.7 ±0.1 rows, respectively; mean ±SEM) and the contralateral control retinas (4.9 ±0.2 rows and 2.7 ±0.2 rows, respectively). A comparison between central and peripheral retinal regions at each age also revealed no significant differences in the number of rows of nuclei between GDNF-treated and control retinas (Fig. 13A). In contrast, the number of rows of photoreceptor nuclei 2 and 4 months old animals treated with CNTF-NSCs (6.5 ±0.1 rows and 3.7 ±0.1 rows, respectively) or GDNF/CNTF-NSCs (6.2 ±0.2 rows and 3.5 ±0.1

rows, respectively) was higher than in the respective control retinas ((4.8 ±0.1 rows and 2.6 ±0.2 rows, respectively) and (4.9 ±0.2 rows and 2.7 ±0.1 rows, respectively; Fig. 13A)). While the difference in the number of rod nuclei was significant in peripheral retinal regions for both treatments and at both ages (Fig. 13B, 13C), there was a trend of higher rod nuclei numbers in central retinal regions (Fig. 13B, 13C) which, however, reached significance only in 2 months old mice treated with CNTF-NSCs (Fig. 13B).

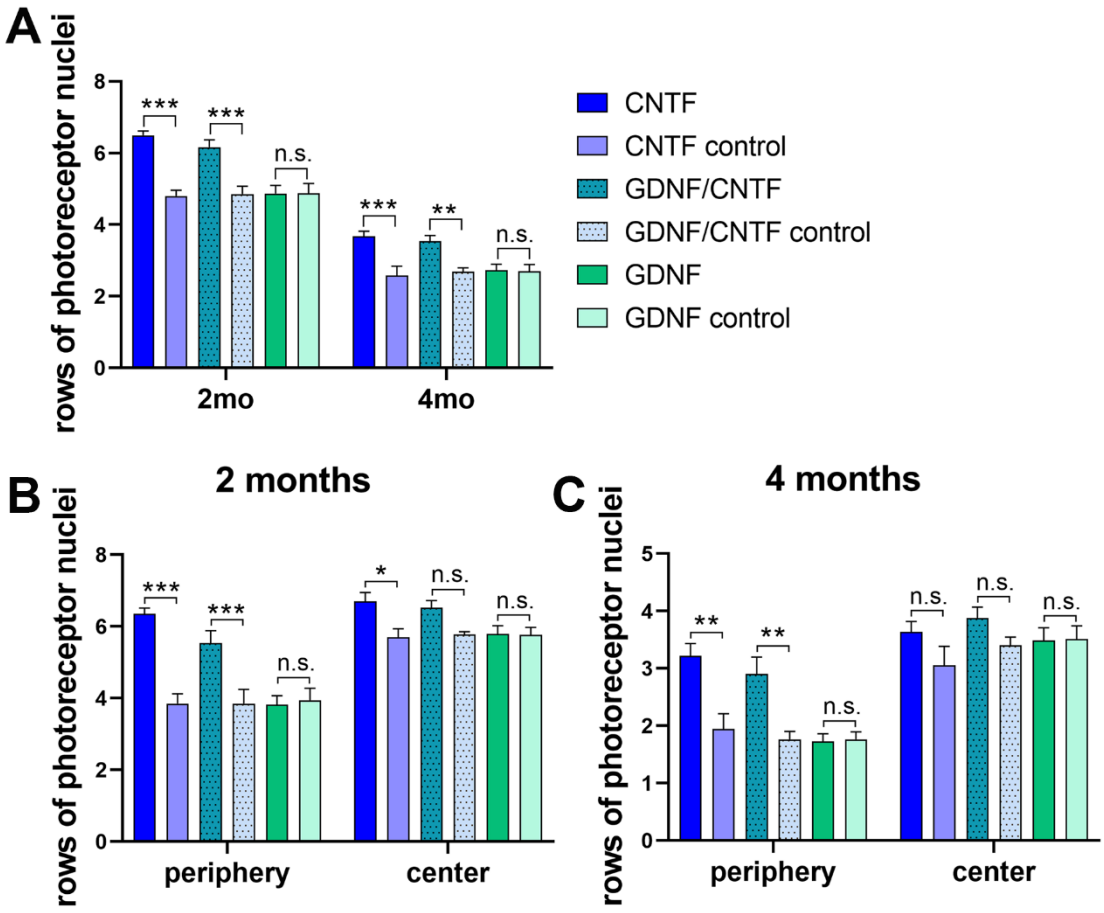

Figure 13: CNTF-NSCs and GDNF/CNTF-NSCs, but not GDNF-NSCs, promote photoreceptor survival.

(A) Analyses of entire retinas revealed a significantly higher number of rows of photoreceptor nuclei in retinas with grafted CNTF-NSCs or GDNF/CNTF-NSCs compared with contralateral control retinas both in 2 months and 4 months old *Cln7* ko retinas. Grafted GDNF-NSCs had no effect on photoreceptor survival. (B, C) The protective effect of CNTF-NSCs and GDNF/CNTF-NSCs was mainly restricted to peripheral retina regions both in 2 months and in 4 months old mutants. Each bar represents the mean value (±SEM) of at least 6 animals. *, $p<0.05$; **, $p<0.01$; ***, $p<0.001$, two-way ANOVA with repeated

measurements followed by Bonferroni 's multiple comparison test.) n.s., not significant.

Cone photoreceptor cells account for about 3% of all photoreceptor cells in the mouse retina, whereas the remaining photoreceptors are rods (Carter-Dawson and LaVail 1979). In 4 months old CLN7 deficient mice, a previous study reported a greater than 70% loss of rod photoreceptor cells but no detectable loss of cone photoreceptor cells (Jankowiak et al. 2016).

In line with this finding, qualitative inspection of retina sections stained with PNA revealed a similar density of cones in GDNF-, GDNF/CNTF- and CNTF-treated retinas and their respective control retinas at both, 2- and 4 months of age (Fig. 14A). Quantitative analyses confirmed similar densities in retinas treated with the different neurotrophic factors and their contralateral control retinas at both ages ($p>0.05$ for all comparisons, two-way ANOVA; Fig. 14B).

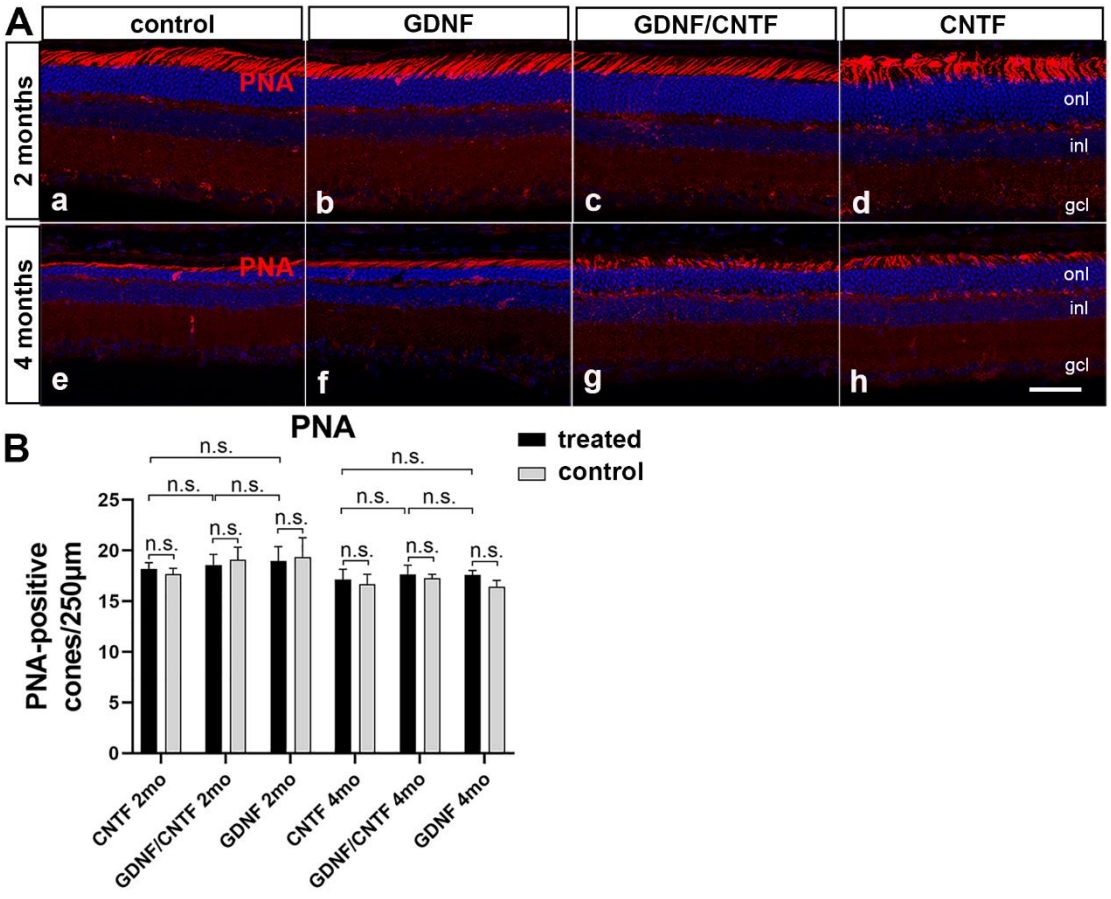

Figure 14: No effect of the neuroprotective treatment on cone photoreceptor survival. (A) The density of peanut agglutinin-labelled cone photoreceptor cells was similar in 2 (a-d) and 4 months old (e-h) *Cln7* ko retinas. Furthermore, there were no differences in the density of cones between retinas with grafted control-NSCs (a, e), GDNF-NSCs (b, f), GDNF/CNTF-NSCs (c, g) and CNTF-NSCs (d, h). (B) Quantitative analyses confirmed

that the number of cone photoreceptors in *Cln7* ko retinas did not differ with respect to age or treatment. Each bar indicates the mean (standard error of the mean) of six animals (B). Two-way ANOVA followed by Tukey's multiple comparison test. gcl, ganglion cell layer; inl, inner nuclear layer; onl, outer nuclear layer; n.s., not significant. Scale bar in (h) for (a-h): 50µm.

Similar to cone photoreceptor cells, there were no obvious differences in the densities of SCGN-positive cone bipolar cells or PKCα-positive rod bipolar cells in GDNF-, GDNF/CNTF- or CNTF-treated retinas and their respective contralateral control retinas, neither at 2 nor at 4 months of age (Fig. 15A). Quantitative analyses confirmed similar numbers of cone and rod bipolar cells in retinas treated with the different neurotrophic factors and the respective control retinas at both ages ($p>0.05$ for all comparisons, two-way ANOVA, Fig. 15Ba, Bb).
(page breaks)

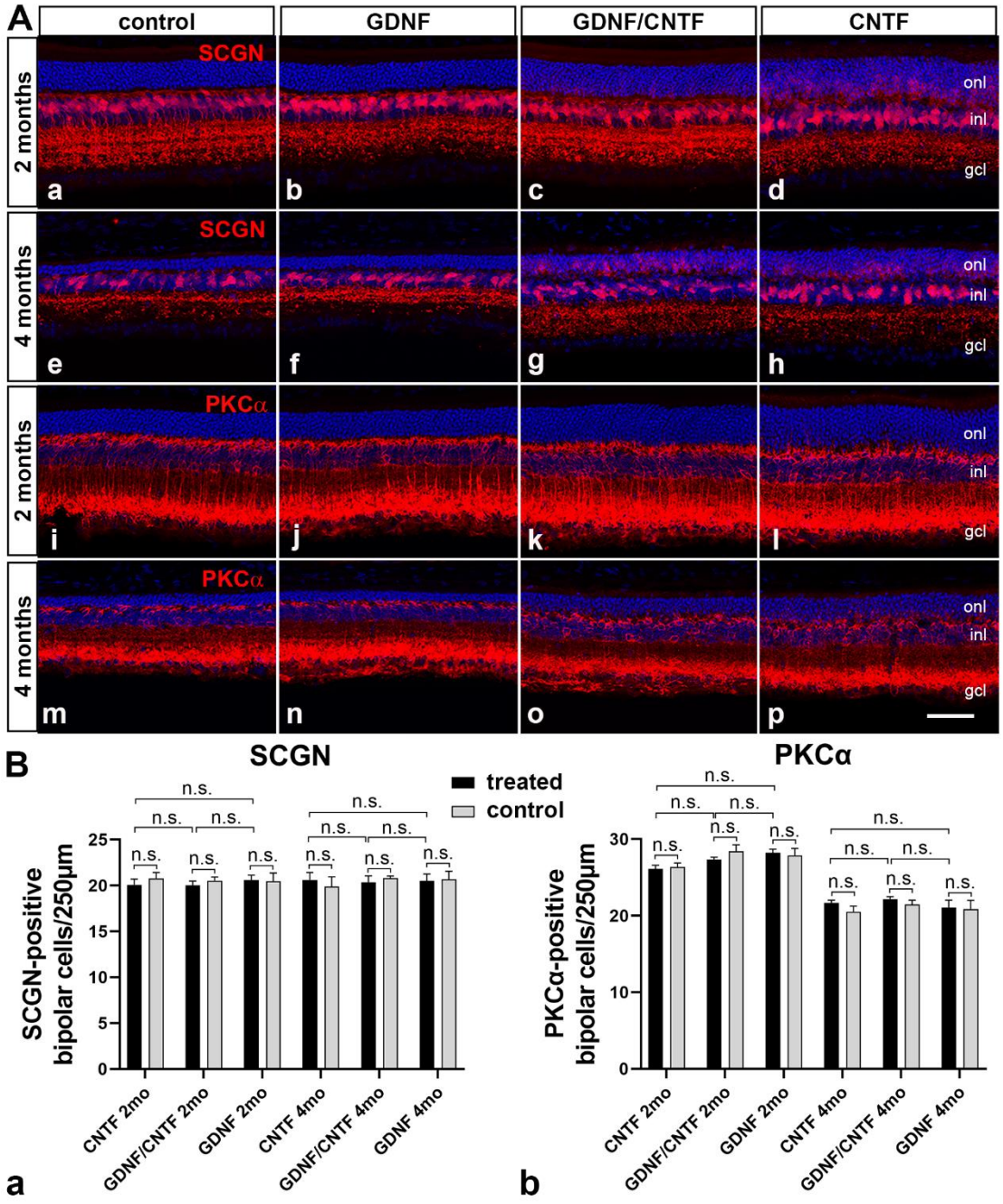

Figure 15: No effect of the neuroprotective treatment on rod or cone bipolar cell survival.

(A) The density of SCGN-positive cone bipolar cells (a-h) and PKCα -positive rod bipolar cells (i-p) were similar in 2 months old (a-d; i-l) and 4 months old (e-h; m-p) *Cln7* ko retinas and in retinas treated with control-NSCs (a, e, i, m), GDNF-NSCs (b, f, j, n), GDNF/CNTF-NSCs (c, g, k, o) or CNTF-NSCs (d, h, l, p). (B) Quantitative analyses confirmed similar numbers of cone bipolar cells (Ba) and rod bipolar cells (Bb) in retinas of different age and retinas with different treatments. Each bar represents the mean value (±SEM) of 6 animals. Two-way ANOVA, followed by Tukey's multiple comparison test. gcl,

ganglion cell layer; inl, inner nuclear layer; onl, outer nuclear layer; n.s., not significant. Scale bar in (p) for (a-p): 50µm.

3.2.6 Impact of the neuroprotective treatment on retina function

Electroretinography (ERG) was performed to evaluate the impact of the sustained intraocular delivery of neurotrophic factors on retinal function in *Cln7* ko mice. CNTF-NSCs treatment resulted in a significantly decreased ERG responses, in line with previous observations in animal models and humans presenting with retinal dystrophies (Wen et al. 2012; Langlo et al. 2015; Liang et al. 2001; Zein et al. 2014; Rhee et al. 2007). Specifically, our ERG recordings reveal a decrease in scotopic and photopic a-waves and b-waves upon CNTF treatment, both at 2 and at 4 months of age (Fig. 16A-D). Similar albeit less pronounced effects were observed in animals treated with GDNF/CNTF-NSCs, with the only exception of the photopic a-wave in 2 months old mutants which was not significantly different from that recorded from the contralateral control retinas (Fig. 16A-D). Amplitudes of scotopic and photopic a-waves in 2 and 4 months old GDNF-treated retinas, in contrast, were similar to those recorded in the respective control retinas (Fig. 16A, 16C). However, amplitudes of scotopic b-waves were reduced in GDNF-treated retinas at 2 and 4 months when compared to control retinas (Fig. 16B) while amplitudes of photopic b-waves were similar in GDNF-treated and control retinas in 2 months old mutants, but reduced when compared to control retinas at 4 months of age (Fig. 16D).

In summary, we found that a sustained intraocular administration of CNTF or GDNF/CNTF had a pronounced negative impact on retina function as assessed in scotopic and photopic ERG recordings. The cell-based intravitreal administration of GDNF, in comparison, had neither a negative nor a positive effect on scotopic or photopic a-wave amplitudes, and an overall minor negative effect on scotopic and photopic b-wave amplitudes.

(page breaks)

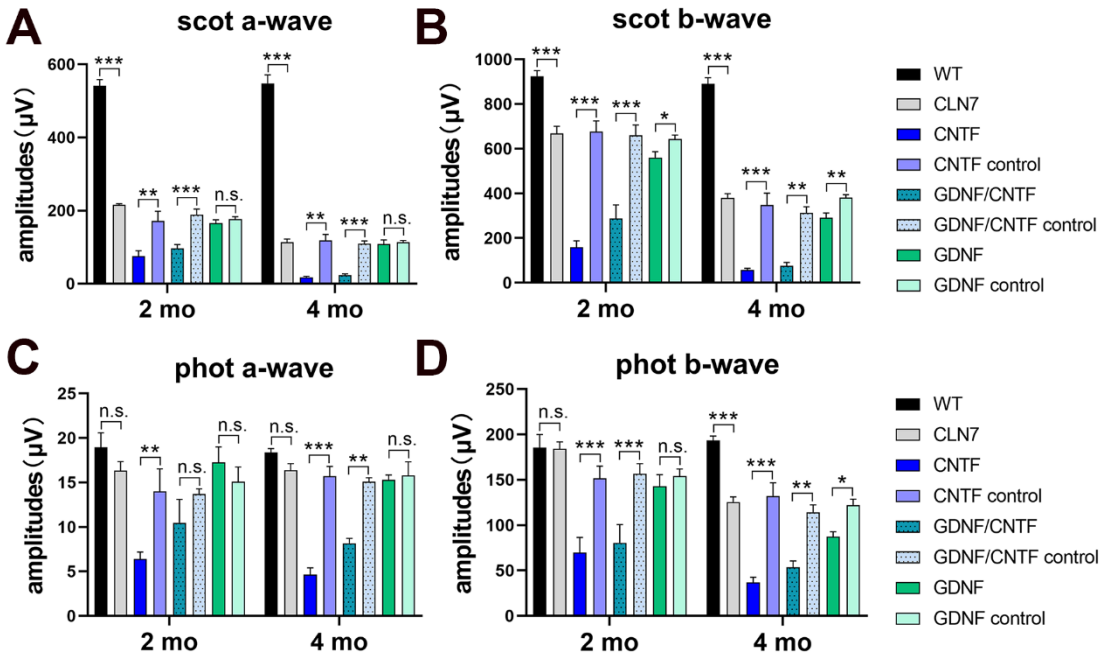

Figure 16: The impact of a sustained intraocular administration of neurotrophic factors on retinal function.

(A, B) Amplitudes of the scotopic a-wave and b-wave were significantly reduced in 2 and 4 months old untreated *Cln7* ko retinas when compared to untreated wild-type retinas. Scotopic a-wave and b-wave amplitudes were also significantly reduced at both ages in retinas treated with CNTF-NSCs or GDNF/CNTF-NSCs when compared to the contralateral eyes treated with control-NSCs. GDNF-NSCs had no effect on the scotopic a-wave amplitude, and a negative effect on the scotopic b-wave amplitude. (C) The photopic a-wave amplitude was not significantly between 2 or 4 months old *Cln7* ko and wild-type retinas. Treatment with CNTF-NSCs had a negative effect on the photopic a-wave amplitude in 2 and 4 months old animals. GDNF/CNTF-NSCs negatively affected the photopic a-wave amplitude in 4 months old mutants but not in 2 months old mutants, while GDNF-NSCs had no effect on the a-wave amplitude. (D) The photopic b-wave amplitude was significantly reduced in 4 months old, but not in 2 months old, untreated *Cln7* ko retinas. CNTF-NSCs and GDNF/CNTF-NSCs negatively impacted the photopic b-wave response in 2 and 4 months old mutants, while GDNF-NSCs had no effect in 2 months old animals, but a negative effect in 4 months old animals. Each bar represents the mean value (±SEM) of at least 6 animals. *, $p<0.05$; **, $p<0.01$; ***, $p<0.001$, n.s., not significant, two-way ANOVA followed by Bonferroni 's multiple comparison test for all comparisons between untreated *Cln7* ko and wild-type animals; two-way ANOVA with repeated measurements followed by Bonferroni 's multiple comparison test for all comparisons between treated and contralateral control retinas.

(page breaks)

4. Discussion

NCL is the umbrella term for a group of neurodegenerative diseases that typically manifest in early childhood. Patients develop widespread neurodegeneration in the brain causing severe symptoms such as seizures, dementia, progressive psychomotor decline and motor deterioration, ultimately resulting in premature death. Retinal degeneration leading to visual failure and blindness is another characteristic clinical feature of most NCLs.

Preclinical work has demonstrated promising therapeutic outcomes of brain- or retina-directed enzyme replacement therapies (ERTs) for NCL forms that are caused by dysfunctions of lysosomal enzymes such as CLN1, CLN2, CLN10 and CLN11(Chang et al. 2008; Hu et al. 2012; Katz et al. 2014; Lu et al. 2015; Marques et al. 2020; Vuillemenot et al. 2015; Whiting et al. 2014; Whiting et al. 2015; Whiting et al. 2020; Whiting et al. 2020; Liu et al. 2022). The efficacy of this treatment is based on the ability of the diseased cells to internalize the injected recombinant enzymes through a receptor-mediated uptake where they are subsequently transported to the lysosomes. An even more pronounced therapeutic benefit was reported in animal models of these NCL forms after a sustained administration of lysosomal enzymes to the diseased nervous tissue, achieved by either a virus-mediated gene transfer or transplantations of cells that were genetically modified to overexpress functional enzymes (Arrant et al. 2018; Cabrera-Salazar et al. 2007; Griffey et al. 2004; Griffey et al. 2005; Griffey et al. 2006; Katz et al. 2015; Liu et al. 2022; Macauley et al. 2012; Shevtsova et al. 2010; Shyng et al. 2017). In comparison, treatment options for NCLs caused by mutations in transmembrane proteins, such as CLN7 disease, are more challenging (see below). Strategies to develop treatments for these NCL forms include corrective gene therapy, small molecule therapy, immunomodulatory therapy or neuroprotective approaches (Kohlschutter et al. 2019).

The present study was performed to extend a previous analysis of the retinal phenotype of the *Cln7* ko mouse (Jankowiak et al. 2016) by analyzing the mutant´s retina at more advanced stages of the disease and by analyzing retina function using ERG recordings. Another aim of the present work was to evaluate the therapeutic potential of a cell-based neuroprotective approach in

preserving retina structure and function. Specifically, we tested the therapeutic impact of the neurotrophic factors CNTF and GDNF which are both known to rescue retinal cell types from cell death.

4.1 The retinal phenotype of *Cln7* knockout mice

CLN7 disease is caused by mutations in a gene encoding an endolysosomal chloride channel (Wang et al. 2021). A mouse model that faithfully recapitulates several clinical features of CLN7 patients has recently been generated (Brandenstein et al. 2016), including retinal degeneration (Jankowiak et al. 2016). A previous study has analyzed the biochemical and morphological characteristics in depth - but not of the functional characteristics - phenotype of the *Cln7* ko retina up to the fourth postnatal month. This work demonstrated early-onset accumulation of lysosomal storage material as indicated by SCMAS and saposin D levels, dysregulation of different lysosomal proteins, a pronounced reactive astrogliosis and microgliosis, and a rapidly progressing loss of rod photoreceptor cells. The present study confirmed all these data and additionally demonstrated accumulation of the autophagy marker SQSTM1/p62 preferentially in the inner nuclear layer, indicative for an impaired autophagic flux. In striking contrast to the study of Jankowiak and colleagues, we also observed a significant loss of cone photoreceptor cells at 4 months of age. Loss of cones was most prominent in peripheral retina regions where it was already evident at 2 months of age. Furthermore, we discovered an early-onset degeneration of rod and cone bipolar cells as well as a considerable decrease in the amount of both types of interneurons in 2 months old retinas. A pronounced reduction of scotopic a- and b-wave amplitudes in 2 months old mutants, followed by significantly reduced amplitudes of the photopic a- and b-wave at later stages of the disease are in line with the loss of rod and cone photoreceptor cells and rod and cone bipolar cells. In summary, the present work demonstrated that *Cln7* ko mice display a more complex retinal dystrophy than previously reported, with an involvement of multiple retinal nerve cell types and a compromised retinal function at early stages of the disease.

4.2 CLN7 patients

CLN7 patients present with complex and variable clinical symptoms. Topcu et al. (Topcu et al. 2004) investigated the clinical and histopathological characteristics of 36 Turkish patients diagnosed with late-infantile NCL. The average age of patients at disease onset was between two and seven years. Seizures and developmental retardation were the most prevalent early clinical signs (Topcu et al. 2004; Kousi et al. 2009). At later stages of the disease, patients presented with progressive cognitive and physical impairment, myoclonus, personality changes, and blindness. A Rett syndrome-like disease onset at 18 months of age has also been reported (Craiu et al. 2015). Of note in the context of this work, the visual impairment clearly preceded the neurological defects in some cases (Topcu et al. 2004; Aldahmesh et al. 2009; Patino et al. 2014; Kousi et al. 2009; Aiello et al. 2009). For instance, visual failure was the initial symptom of a 11 years old patient, while motor impairment, seizures, and ataxia emerged later at the age of 24, 25, and 28 years, respectively (Kousi et al. 2009). Mental and verbal regression became evident at the age of 30 and 36 years respectively, and this individual became wheelchair bound at the age of 39 years. Early-onset retinal degeneration and visual impairment in CLN7 patients is faithfully recapitulated in *Cln7* ko mice where retinal degeneration and retinal dysfunction precedes other neurological defects (Jankowiak et al. 2016; Brandenstein et al. 2016), confirming that the mutant mouse represents a useful animal model for this disease. Recently, *MFSD8* mutations were identified that cause non-syndromic autosomal recessive macular dystrophy or generalized retinopathy (Khan et al. 2017; Roosing et al. 2015; Birtel et al. 2018; Poncet et al. 2022). Genotype–phenotype demonstrated that vLINCL and non-syndromic retinal degeneration are not distinct disease entities but rather phenotypic variations caused by mutations in the same gene (Roosing et al. 2015; Zare-Abdollahi et al. 2019; Khan et al. 2017; Poncet et al. 2022). While a compound heterozygous condition with a severe (i.e., nonsense or frameshift) and a moderate pathogenic (missense) mutation in *MFSD8* resulted in non-syndromic retinal degeneration, two severe mutations resulted in vLINCL. In summary, involvement of the retina early in the course of the disease and rare cases of

non-syndromic retinal dystrophies indicate that the retina is particularly vulnerable to lysosomal dysfunction caused by mutations in the *MFSD8* gene.

4.3 Neural stem cell-based neuroprotection as a strategy to treat retinal degeneration in CLN7 disease

As indicated above, it has recently been shown that CLN7 is an endolysosomal chloride channel (Wang et al. 2021). The development of treatment options for NCL forms caused by defective intracellular transmembrane proteins is a challenging task. One potential strategy is corrective gene therapy. In fact, an adeno-associated virus (AAV) vector-mediated gene transfer of *Mfsd8* to the brain of *Cln7* ko mice resulted in therapeutic benefits, such as reduction of storage material, normalization of behavioral deficits and an extended life span of the mutant (Chen et al. 2022). In the present work, we analyzed the efficacy of a neural stem cell-based intraocular administration of neurotrophic factors in attenuating retinal degeneration in the *Cln7* ko mouse. We focused on ciliary neurotrophic factor (CNTF) and glial cell line-derived neurotrophic factor (GDNF) which both are known to rescue photoreceptor cells and retinal ganglion cells.

CNTF has been shown to promote the survival of photoreceptors in animal models of various retinal dystophies (Wen et al. 2012; Lipinski et al. 2015; Jung et al. 2013), including CLN6 disease (Jankowiak et al. 2015). Binding of CNTF to a receptor complex composed of membrane-bound or soluble CNTF receptor α (CNTFRα) and the signal transducing receptors gp130 and leukemia inhibitory factor receptor (LIFR) initiates signaling cascades such as the Janus kinase/signal transducer and activator of transcription (JAK/STAT), mitogen-activated protein kinase (MAPK) and phosphoinositide 3-kinase (PI3K) pathways (Zheng et al. 2018). Using a genetic approach, it has been demonstrated that exogenous recombinant human CNTF protects photoreceptors through initial signaling via the gp130 receptor in Müller glia (Rhee et al. 2013).

Similar to CNTF, GDNF has also been shown to attenuate photoreceptor degeneration under pathological conditions and to preserve retinal function (Touchard et al. 2012; Garcia-Caballero et al. 2018; Baranov et al. 2017; Wong

et al. 2016). GDNF interacts with the GDNF family receptor alpha-1 (GFRα1) (Jing et al. 1996; Treanor et al. 1996) and exerts its biological effects via interaction of the GDNF–GFRα1 complex with the membrane-bound tyrosine kinase receptor RET (Takahashi and Cooper 1987). While GDNF–GFRα1 appears to be the primary connection, GDNF signaling can alternatively be mediated through interactions of a GDNF–GFRα2 complex with RET (Sanicola et al. 1997) or through interactions of GDNF–GFRα1 with a transmembrane or linker protein other than RET (Trupp et al. 1999). The GDNF receptors GFR-α1 (Harada et al. 2002; Harada et al. 2003; Koeberle and Ball 2002; Jomary et al. 1999; Hauck et al. 2006), GFR-α2 (Harada et al. 2002; Harada et al. 2003) and RET (Jomary et al. 1999) have been identified on photoreceptors and retinal Müller cells. Thus, GDNF may exert its protective effects on photoreceptor cells either directly or indirectly via Müller cells (Jing et al. 1996; Politi et al. 2001; Carwile et al. 1998).

It is well established that CNTF and GDNF not only promote survival of photoreceptor cells (Buch et al. 2006; Cayouette and Gravel 1997; Chong et al. 1999; Huang et al. 2004; Jankowiak et al. 2015; Liang et al. 2001; Lipinski et al. 2015; Carwile et al. 1998; Dalkara et al. 2011; Del Rio et al. 2011; Gregory-Evans et al. 2009; McGee Sanftner et al. 2001; Wong et al. 2016) but also of retinal ganglion cells (Yan et al. 1999; Ward et al. 2007; van Adel et al. 2005; Leaver et al. 2006; Koeberle and Ball 1998; Klocker et al. 1997; Ji et al. 2004; Ishikawa et al. 2005; Hellstrom et al. 2011; Flachsbarth et al. 2014; Checa-Casalengua et al. 2011; Jiang et al. 2007). Of particular relevance in the context of this thesis, our group has recently shown that a co-administration of GDNF and CNTF exerts pronounced synergistic neuroprotective effects on axotomized retinal ganglion cells over a time period of up to 8 months after the optic nerve lesion (Flachsbarth et al. 2018; Dulz et al. 2020). Notably, the co-administration of both factors resulted in the survival of almost 5-fold more axotomized ganglion cells 8 months after the optic nerve lesion than treatments with each factor alone (Dulz et al. 2020). It remains to be clarified whether this marked synergistic protective effect is mediated by direct (i.e. via their cognate receptors) or indirect (e.g. via induction of additional neurotrophic factors in Müller cells) effects, or both.

Based on all the data discussed above, we tested the therapeutic potential of either CNTF or GDNF or the combination of both neurotrophic factors in

attenuating the morphological and functional phenotype of the *Cln7* ko retina.

4.4 Sustained neural stem cell-based administration of neuroprotective factors to the *Cln7* knockout retina

The development of neuroprotective treatments with neurotrophic factors is faced with the problems that these factors (i) usually have a short half-life and (ii) can not penetrate the blood-retina barrier. The development of such treatments therefore requires a methodology which allows a sustained and local delivery of neurotrophic factors (Birch et al. 2016; Birch et al. 2013; Bush et al. 2004; Kauper et al. 2012; Sieving et al. 2006; Zhang et al. 2011). In preclinical studies, these aims have been successfully achieved with virus-mediated gene transfer technologies (Ghasemi et al. 2018; Schmeer et al. 2002; Dalkara et al. 2011), implantations of growth factor-loaded slow-relase devices (Thanos et al. 2004; Emerich and Thanos 2008; Kauper et al. 2012; Zhang et al. 2011; Wong et al. 2017; Wahlberg et al. 2020; Sieving et al. 2006) or transplantations of genetically modified cells that overexpress distinct neurotrophic factors (Lawrence et al. 2004; Gamm et al. 2007; MacDonald et al. 2007; Gregory-Evans et al. 2009; Hu et al. 2017). In the present study we employed the latter approach, and used previously established clonal neural stem cell lines with an overexpression of either GDNF or CNTF. To co-administer both factors, we co-transplanted a 1:1 mixture of the GDNF- and the CNTF-expressing cell line. Importantly, we used cell lines that have been shown in previous studies to effectively rescue photoreceptor cells in mouse models of RP (Jung et al. 2013) or CLN6 disease (Jankowiak et al. 2015), and RGCs in an optic nerve crush model (Flachsbarth et al. 2014; Flachsbarth et al. 2018; Dulz et al. 2020).

One reason to select a cell-based delivery strategy was the principal possibility to transfer the approach to clinical applications, as demonstrated by the so-called encapsulated cell technology (ECT). ECT uses an encapsulated retinal pigment epithelial cell line (ARPE-19) genetically modified to overexpress CNTF. The encapsulated cells were implanted into the vitreous cavity of patients with geographic atrophy, retinitis pigmentosa or macular telangiectasia type 2. The clinical trials reported only minimal adverse effects of the cell implants and some therapeutic effects such as a long-term protection of cone

photoreceptor cells. Important aspects of this treatment strategy include the possibility to adjust the amount of neurotrophic factors secreted from the cell capsules prior to intravitreal implantation, or to explant the cell implants in case of complications (Zhang et al. 2011; Talcott et al. 2011; Sieving et al. 2006; Kauper et al. 2012; Chew et al. 2019; Birch et al. 2016).

4.5 Survival, differentiation and transgene expression of transplanted neural stem cells

Analyses of GDNF/CNTF-NCSs treated eyes 3.5 months after cell transplantation indicated the presence of abundant donor cells that had established compact density cell layers on the posterior poles of the lenses and co-expressed either eGFP and GDNF or Venus and CNTF, which was consistent with previous studies, although the time points analyzed after transplantation varied from P8 (Jung et al. 2013) to P16 (Jung et al. 2013), P42 (Jankowiak et al. 2015), P56 (Flachsbarth et al. 2018), P112 (Flachsbarth et al. 2014), and even P224 (Dulz et al. 2020). No adverse effects of integrate the transplanted cells into host retina or tumor formation were observed in any experimental animal, consistent with the fact that NSCs cease proliferation swiftly following intravitreal transplantation (Jung et al. 2013). Almost all control-NSCs differentiated into GFAP-positive astrocytes, as previously reported (Jung et al. 2013; Flachsbarth et al. 2014; Jankowiak et al. 2015; Flachsbarth et al. 2018; Dulz et al. 2020), whereas GDNF/CNTF-NSCs differentiated into GFAP-positive astrocytes as well as β-tubulin III-positive neurons with a dense network of neurites in line with this research (Dulz et al. 2020). We believe it is more plausible that that a large proportion of NSCs develop into neurons right after transplantation, with CNTF alone having a limited rescue capacity, whereas GDNF has none, and the combination of CNTF and GDNF has a synergistic rescue capacity to save these neurons from cell death. NSC cultures are composed of a homogenous population of tripotent stem cells that have a high potential for neuronal differentiation after lengthy passage (Conti et al. 2005; Pollard et al. 2006; Glaser et al. 2007). After a further 19 passages, similar quantities of CNTF were secreted in the CNTF-NSC line (Flachsbarth et al. 2014), whereas similar levels of GDNF were secreted in the GDNF-NSC line

after an additional 21 passages (Flachsbarth et al. 2018), demonstrating sustained expression of both factors.
In summary, robust survival and sustained expression of transgenes in NSC-derived donor cells were observed in accordance with previous studies (Jung et al. 2013; Flachsbarth et al. 2014; Jankowiak et al. 2015; Flachsbarth et al. 2018; Dulz et al. 2020).

4.6 Treatment effect on storage material accumulation, lysosomal protein dysregulation and neuroinflammation

The accumulation of intracellular autofluorescent storage material is a hallmark of all NCL forms, and is discussed as the direct cause of the neurodegeneration underlying these diseases. Previous biochemical analyses demonstrated that the storage material in CLN7-deficient retinas (Jankowiak et al. 2016) and brains (Brandenstein et al. 2016) contains both SCMAS and Saposin D. A pronounced dysregulation of various lysosomal proteins and reactive astrogliosis and microgliosis were identified as other hallmarks of the retinal dystrophy in *Cln7* ko mice (Jankowiak et al. 2016). Furthermore, upregulation of the autophagy marker sequestosome 1 (SQSTM1)/p62 indicated a disrupted autophagic flux. In this study, we observed a similar intensity and distribution of the immunoreactive signals for LAMP1, LAMP2, CTSD, CTSZ, saposin D, SCMAS, Iba1 and CD68 in CNTF-, GDNF- and GDNF/CNTF-treated retinas compared to the respective contralateral control retinas, indicating that a sustained intraocular administration of these neuroprotective factors exhibited no favorable effect on the dysregulated expression of lysosomal proteins, storage material accumulation, reactive astrogliosis and microgliosis, or the defective autophagic flux.
Transplantations of CNTF-NSCs into CLN7-deficient retinas resulted in 35.4% and 42.3% more rows of photoreceptor nuclei compared to the contralateral control retinas at 2 and 4 months of age, respectively. Although the protective effect of the CNTF-NSCs on photoreceptor cell survival in *Cln7* ko mice was observed in all regions of the experimental retina, we found a considerably greater protective effect in the peripheral regions of the retinas than in central regions of the retina, probably because the more severe degeneration in the

periphery. The neuroprotective effect of CNTF on photoreceptors observed in the *Cln7* ko retina is consistent with reports on animal models of other retinal dystrophies (Liang et al. 2001; Bok et al. 2002; Wen et al. 2006; Rhee et al. 2007; Talcott et al. 2011; Zhang et al. 2012; Jankowiak et al. 2016). The therapeutic effect on photoreceptors was evident for up to 3.5 months after transplantation, significantly longer than the 6 week-interval observed in a mouse model of CLN6 disease after intravitreal transplantation of the same CNTF NSC clone (Jankowiak et al. 2016). However, transplantation of CNTF-NSCs showed neither a morphological nor a functional benefit on cone photoreceptors, which is in agreement with the finding that intravitreal injections of purified CNTF can prevent the death of rods, but not that of cones in the *Pde6b*^{rd1} mouse, an animal model of RP (LaVail et al. 1998). Transplantation of CNTF-NSCs had no protective impact on rod and cone bipolar cells as well. Furthermore, despite the remarkable preservation of photoreceptors intravitreally delivered CNTF-secreting NSCs did not result in improved photopic or scotopic ERG responses, but rather resulted in decreased ERG amplitudes, in line with previous studies (Bok et al. 2002; Liang et al. 2001; Schlichtenbrede et al. 2003; Rhee et al. 2013). The first explanation for this paradoxcial observation is that CNTF protects photoreceptor cells, at least in part, indirectly by stimulating retinal Müller cells to release a variety of other neuroprotective factors, including FGF-2. CNTF has also been found to stimulate RPE cells to release FGF-2 (Hackett et al. 1997). Of note, FGF-2 has an inhibitory effect on photoreceptor function. For example, AAV-mediated administration of FGF-2 to S334ter heterozygous rhodopsin transgenic rats revealed histological evidence of photoreceptor protection, but retinal function did not exhibit similar protection (Lau et al. 2000). FGF-2 also showed suppression of b-wave amplitudes in rat retinas (Gargini et al. 1999). The second possibility is that CNTF directly impairs photoreceptor function. McGill et al. discovered that whereas intravitreal injections of high CNTF doses of up to 10 microgram and subretinal injections of CNTF encoding AAV vectors lowered ERG amplitudes in rats, this was not the case with low CNTF doses (1–100 ng) (McGill et al. 2007). In rabbits, an electroconvulsive therapy (ECT)-based method resulted in dose-dependent alterations in nuclear morphology, in addition to a decline in the cone b-wave amplitude. Similar results were

reported when normal rabbit retinas were exposed to high doses of intravitreally implanted CNTF-secreting encapsulated cells (Bush et al. 2004). Different studies have provided evidence that CNTF induces a variety of biochemical and morphological alterations in rod photoreceptors, including an irregular shape of the rod outer segments, a greater distance between rod outer segments and disorganized disks, all of which result in a decrease in photoresponsiveness. Consequently, the amplitudes of a- and b-waves are reduced for a given stimulus intensity in retinas treated with CNTF (Wen et al. 2006). Furthermore, Overexpression of CNTF may also drive inner retinal remodeling, resulting in a change in synaptic architecture. In the process of retinal degeneration, loss of photoreceptor input is thought to result in morphological alterations of secondary neurons in the inner retina. Anatomical changes at the synaptic level as well as variations in the function of Müller cells might contribute to the impaired photoreceptor function in CNTF-treated retinas. A previous study has shown that the CNTF dosage and the duration of the CNTF therapy impact the function of the restored neurons significantly. However, Lipinski et al. (Lipinski et al. 2015) demonstrated that despite inhibition of electrophysiological function of photoreceptors as measured by ERG, hCNTF-mediated neuroprotective effects resulted in improved vision at late disease stages as measured by optomotor responses and laser speckle imaging (LSI) in the visual cortex. CNTF administered by an intraocular encapsulated cell technology implant appears to delay the course of vision loss in geographic atrophy patients, particularly in eyes with 20/63 vision or at a better baseline (Zhang et al. 2011). Similar to the CNTF-NSCs-treated retinas, GDNF/CNTF-NSCs-treated retinas also showed a better survival of photoreceptors and decreased responses in photopic and scotopic ERG recordings, albeit the effects were not as pronounced as in the CNTF group. It is likely that both effects are mediated by CNTF in the GDNF/CNTF-treated retinas. It is also reasonable to speculate that the slightly less pronounced effects are due to the fact that the number of transplanted CNTF-expressing cells in the GDNF/CNTF group accounts for only 50% of the number of CNTF-expressing cells transplanted into retinas treated with CNTF only. Specifically, transplantation of GDNF/CNTF-NSCs resulted in 26.5% and 29.6% more rows of photoreceptor nuclei compared to contralateral control retinas at 2 and 4 months of age, respectively. Similar to

the CNTF group, there was no protective effect of the GDNF/CNTF treatment on rod and cone bipolar cells. Importantly, our group used the same clonal cell lines to co-administer GDNF and CNTF to the retina of a glaucoma mouse model. Interestingly, both factors together conferred a pronounced protective effect to retinal ganglion cells that lasted for up to 8 months after the cell transplantation (Flachsbarth et al. 2018; Dulz et al. 2020). In contrast, there was no cooperative, additive or synergistic neuroprotective effect on photoreceptors. On the contrary, photoreceptor survival in GDNF/CNTF-treated retinas was less pronounced than in retinas treated with CNTF only. The reason for the discrepant effects of a combined administration of GDNF and CNTF on retinal ganglion cells and photoreceptor cells are unknown. GDNF and CNTF both induce the secretion of other neurotrophic factors from Müller cells (Rhee et al. 2013; Hauck et al. 2006; Harada et al. 2003; Del Rio et al. 2011), and it might be speculated that induced Müller cells release neuroprotective factors that preferentially promote the survival of ganglion cells rather than of photoreceptor cells.

An unexpected finding of the present study was that intravitreally delivered GDNF had no protective effect on photoreceptor cells and no therapeutic impact on retina function. This finding contrasts with previous publications showing that GDNF slows photoreceptor degradation and maintains retinal function in animal models of multiple retinal dystrophies (Dalkara et al. 2011; Frasson et al. 1999; McGee Sanftner et al. 2001). For example, AAV-mediated GDNF secretion from photoreceptors slowed disease progression in a rat model of RP, as indicated by electroretinography (ERG) and histology (McGee Sanftner et al. 2001). Subretinal injections of peptide for ocular delivery (POD) nanoparticles loaded with recombinant GDNF improved photoreceptor survival in the superior hemisphere by 39.3% and showed a 32% and 27% increase in scotopic a-wave and b-wave amplitudes respectively when compared to buffer injected eyes in adult mice 7 days after light-induced damage (Read et al. 2010). Furthermore, AAVshH10 vector-medicated expression of GDNF in retinal glia cells significantly slowed retinal degeneration in a rat model of RP, and effectively preserved retinal function (Dalkara et al. 2011). Promotion of photoreceptor survival by GDNF has also been reported in rhodopsin-deficient mice (Garcia-Caballero et al. 2018), a rat model of retinal detachment (Wu et

al. 2002) and the rhodopsin TgN S334ter-4 rat model of RP (Gregory-Evans et al. 2009). We cannot fully exclude the possibility that the amount of GDNF delivered to the *Cln7* ko retina in our experiments was not sufficient to protect photoreceptor cells from degeneration. However, we consider this possibility as unlikely because we found a pronounced and long-lasting protection of axotomized retinal ganglion cells after intravitreal transplantations of the same GDNF expressing clonal NSC line in a mouse glaucoma model (Flachsbarth et al. 2018; Dulz et al. 2020). Given that the therapeutic benefit of GDNF for neurodegenerative retinal diseases involving photoreceptors was minor in some of the studies discussed above, we suggest that the relevance of this neurotrophic factor for treatments of such diseases needs careful reconsideration.

4.7 Other therapeutic strategies for the treatment of neurodegeneration in CLN7 disease

Up to now, there are only a few preclinical studies that have focused on the development of treatment options for neurodegeneration in CLN7 disease. A recent study has shown that intraperitoneal administration of tamoxifen reduced accumulation of globotriaosylceramide (Gb3) and SCMAS in the brain of *Cln7* ko mice, and attenuated microglia activation. Of note, the treatment improved motor coordination as measured in a rotarod test and as indicated by hindlimb clasping behavior. The study demonstrated that the effect of tamoxifen was mediated through activation of the transcription factor EB (TFEB), a master gene involved in lysosomal function and autophagy (Soldati et al. 2021). Another recent study showed that intrathecal administration of *AAV9/MFSD8* to *Cln7* ko mice at P7-10 with a single high ($5x10^{11}$ vg) dose resulted in decreased SCMAS accumulation and GFAP immunoreactivity, increased median lifespan, normalization of body weight, and restoration of the impaired behavioral phenotype. In primary fibroblasts from a CLN7 patient, the *AAV2/MFSD8* vector restored lysosomal function. The FDA authorized the investigational new drug (IND) application #19766 in December 2020 to commence a Phase I intrathecal gene transfer trial with *AAV9/MFSD8* (Chen et al. 2022). Considering the retina's susceptibility to lysosomal dysfunction caused by CLN7 protein

dysfunctions, research is urgently required to develop treatments for retinal degeneration in addition to neurodegeneration in the brain.

Rapidly progressive degeneration of photoreceptor cells is the predominant phenotypic feature in both the *Cln6* and *Cln7* mouse model, in a *Cln6* mouse model, photoreceptor cells are the first cells that are lost (Bartsch et al. 2013; Mirza et al. 2013). However, targeting retinal photoreceptors with an AAV2/8-CLN6 vector encoding CLN6 failed to protect photoreceptors from cell death in this mouse model. Instead, targeting bipolar cells with an AAV2/2 variant 7m8 vector preserved photoreceptor morphology and function (Kleine Holthaus et al. 2018). The results indicate that photoreceptor degeneration in the *Cln6* animal models is secondary to a defect in bipolar cells. Notably, degeneration of bipolar cells begins only after a considerable proportion of photoreceptor cells is lost in this animal model. This prompts the working hyposthesis of whether targeting bipolar cells with a viral vector encoding CLN7 may protect photoreceptor cells in *Cln7* ko mouse model, as has been demonstrated in the *Cln6* mouse model.

In conclusion, this is the first study demonstrating degeneration of cone photoreceptor cells and rod and cone bipolar cells in addition to rod photoreceptor cells in a mouse model of CLN7 disease. Furthermore, this study provides the first data on deterioration of retinal function in photopic and scotopic ERG recordings in this mouse model. Neural stem cell-based intravitreal delivery of CNTF resulted in preservation of rod photoreceptors cells. However, a combined cell-based administration of GDNF and CNTF did not exert additive or synergistic protective effects on photoreceptor cells, in striking contrast to previous results on retinal ganglion cells. Interestingly, intravitreal administration of GDNF had no positive therapeutic effects, neither on retinal morphology nor on retina function. This observation is in contrast to other publications demonstrating therapeutic benefit of GDNF administration in animal models of retinal dystrophies.

5. Summary

Neuronal ceroid lipofuscinosis (NCL) is an umbrella term for a group of rare neurodegenerative lysosomal storage disorders. Patients display a variety of severe neurological symptoms and usually die prematurely. Loss of vision is among the characteristic symptoms of most NCL forms including CLN7 disease. *Cln7* knockout (ko) mice represent a model for this disease. The mutant recapitulates many aspects of the human disease, including retinal degeneration. The aim of the present work was to extend a previous phenotypic characterization of the *Cln7* ko retina and to evaluate the therapeutic potential of a neural stem cell- (NSC) based neuroprotective approach in attenuating the retinal dystrophy in this animal model. The present study confirmed previous reports showing an early-onset accumulation of lysosomal storage material, a dysregulation of various lysosomal proteins, a pronounced reactive astrogliosis and microgliosis, a disrupted autophagy, and a rapidly progressing loss of rod photoreceptor cells. In addition, this work demonstrated for the first time an early-onset degeneration of cone photoreceptor cells and rod and cone bipolar cells. A pronounced reduction of the responses in scotopic and photopic electroretinogram recordings (ERGs) is in line with the loss of rod and cone photoreceptor cells and rod and cone bipolar cells.

A sustained administration of the neuroprotective factors ciliary neurotrophic factor (CNTF), glial cell line-derived neurotrophic factor (GDNF), or both (GDNF/CNTF) via intravitreal transplantations of lentivirally modified clonal neural stem cell lines had no effect on storage material accumulation, lysosomal hypertrophy, neuroinflammation or the disrupted autophagy. However, CNTF – and to a lesser extent GDNF/CNTF – promoted rod photoreceptor survival, but not cone photoreceptor or bipolar cell survival. Despite this positive therapeutic effect, both treatments resulted in impaired retina function as assessed in ERGs. In striking contrast to previous studies done on animal models of other retinal dystrophies, intravitreal administration of GDNF had no beneficial effects on retinal degeneration in *Cln7* ko mice, but instead exerted negative effects on scotopic and photopic b-wave amplitudes.

6. Zusammenfassung

Neuronale Ceroid-Lipofuszinose (NCL) ist der Sammelbegriff für eine Gruppe seltener neurodegenerativer lysosomaler Speichererkrankungen. Die Patienten leiden unter verschiedenen schweren neurologischen Symptomen und versterben gewöhnlich frühzeitig. Ein Visusverlust gehört bei den meisten NCL Formen – wie auch der CLN7 Erkrankung - zu den typischen Symptomen. Die *Cln7* knockout (ko) Maus stellt ein Modell für diese Erkrankung dar. Die Mutante rekapituliert verschiedene Merkmale der humanen Erkrankung, einschließlich einer retinalen Degeneration. Ziel dieser Arbeit war es, eine frühere phänotypische Charakterisierung der *Cln7* ko Retina zu vertiefen, und das therapeutische Potential eines Stammzell-(NSC) basierten neuroprotektiven Ansatzes zur Behandlung der retinalen Dystrophy zu überprüfen. Die vorliegende Arbeit bestätigt frühere Berichte, die eine früh einsetzenden Anreicherung von lysosomalen Speichermaterial, eine Dysregulation lysosomaler Proteine, eine ausgeprägte reaktive Astrogliose und Mikrogliose, eine gestörte Autophagie und eine schnelle Degeneration von Stäbchen-Photorezeptoren gezeigt haben. Außerdem weist diese Arbeit zum ersten Mal eine früh einsetzende Degeneration von Zapfen-Photorezeptoren und von Stäbchen- und Zapfen-Bipolarzellen nach. Eine ausgeprägte Reduktion der Antworten in skotopischen und photophischen Elektroretinogramm- (ERG) Ableitungen steht im Einklang mit dem Verlust von Stäbchen- und Zapfen-Photorezeptoren und Stäbchen- und Zapfen-Bipolarzellen.

Eine kontinuierliche Applikation der neuroprotektiven Faktoren „ciliary neurotrophic factor“ (CNTF), „glial cell line-derived neurotrophic factor“ (GDNF) oder eine Ko-Applikation beider Faktoren (GDNF/CNTF) über intravitreale Transplantationen lentiviral modifizierter neuraler Stammzellklone hatte keinen Effekt auf die Akkumulation von Speichermaterial, die lysosomale Hypertrophie, die Neuroinflammation oder die gestörte Autophagie. Dagegen förderte CNTF– und ein einem geringeren Umfang GDNF/CNTF– das Überleben von Stäbchen-Photorezeptoren, aber nicht das Überleben von Zapfen-Photorezeptoren oder Bipolarzellen. Trotz dieses positiven therapeutischen Effekts hatten beide Behandlungen einen negativen Effekt auf die retinale

Funktion. Im Widerspruch zu früheren Studien in Tiermodellen für andere retinale Dystrophien hatte GDNF keinen therapeutischen Effekt auf die retinale Degeneration in der *Cln7* ko Maus. Vielmehr wurden negative Effekte auf die Amplituden der b-Welle in skotopischen und photopischen ERGs beobachtet.

7. List of abbreviations

AAV	adeno-associated viruses
ANOVA	analysis of variance
ARTN	artemin
ASO	antisense oligonucleotide
ATP13A2	ATPase Cation Transporting 13A2
bFGF	basic fibroblast growth factor
BSA	bovine serum albumin
CAG	cytomegalovirus enhancer/chicken ß-actin
CBA	chicken β-actin
CCMD	Chinese classification of mental disorders
CD68	cluster of differentiation 68
CMV	cytomegalovirous
CNTF	ciliary neurotrophic factor
CNTFRα	CNTF receptor α
CTSD	cathepsin D
CTSZ	cathepsin X/Z/P
DA	dark adapted
DAPI	4',6-diamidino-2-phenylindole
DHA	docosahexaenoic acid
DNA	deoxyribonucleic acid
ECT	electroconvulsive therapy
EGFR	*epidermal growth factor receptor*
ER	endoplasmic reticulum
ERG	electroretinogram
ERT	enzyme replacement therapy
ESC	embryonic stem cell
GCL	ganglion cell layer
FAF	fundus autofluorescence
FDA	food and drug Administration
ffERG	full field electroretinogram
FP	fingerprint

GDNF	glial cell line-derived neurotrophic factor
GFAP	glial fibrillary acidic protein
GFL	GDNF family ligand
GFP	green fluorescent protein
GFRα1	GDNF family receptor alpha-1
GLAST	L-glutamate/L-aspartate transporter
GROD	granular osmiophilic deposits
i.c.v.	intracerebroventricular
IBA1	ionized calcium-binding adapter molecule 1
IND	investigational new drug
INL	inner nuclear layer
JAK	Janus kinase
ko	knockout
LAMP1	lysosomal-associated membrane protein 1
LAMP2	lysosomal-associated membrane protein 2
LIFb	leukaemia inhibitory factor receptor b
LIFR	leukaemia inhibitory factor receptor
LSI	laser speckle imaging
MAPK	mitogen-activated protein kinase
MeCP2	methyl-CpG-binding protein 2
mES	mouse embryonic stem
MFSD8	major facilitator superfamily domain containing 8
mRNA	messenger ribonucleic acid
MSs	microspheres
mTOR	mechanistic Target of Rapamycin
n.a.	not applicable
n.s.	not significant
NCL	neuronal ceroid lipofuscinosis
NRTN	neurturin
NSCs	neural stem cells
NTFs	neurotrophic factors
ONH	optic nerve head
ONL	out nuclear layer
OP	oscillatory potentials

OPL	outer plexiform layer
OPN	osteopontin
OS	outer segments
P	postnatal day
PBS	phosphate buffered saline
PCR	polymerase chain reaction
PDE6B	phosphodiesterase 6B
PA	paraformaldehyde
PFKFB3	6-Phosphofructo-2-Kinase/Fructose-2,6-Biphosphatase 3
pH	potential of hydrogen
PI3K	phosphoinositide 3-kinase
PKCα	protein kinase C alpha
PLGA	poly (lactic-co-glycolic) acid
PNA	peanut agglutinin
POD	peptide for ocular delivery
PPT1	palmitoyl-protein thioesterase 1
PRPH	peripherin
PSPN	persephin
RCS	Royal College of Surgeons
RD	retinal detachment
RET	rearranged during transfection
RGCs	retinal ganglion cells
RHO	rhodopsin gene
RL	rectilinear
RMG	retinal Mueller glial cells
RP	retinitis pigmentosa
RPE	retinal pigment epithelium
saposin D	sphingolipid activating proteins D
SCGN	secretagogin
SCMAS	subunit c of mitochondrial ATP synthase
SCTM41	retrovirus-engineered Schwann cell line
SOCS	suppressor of cytokine signaling
SQSTM1/p62	sequestosome 1/p62
STAT	signal transducer and activator of transcription

TFEB	transcription factor EB
TGF-β	transforming growth factor-β
TPPT1	tripeptidyl peptidase 1
TRPML1	transient receptor potential mucolipin 1
VitE	vitamin E
vLINCL	variant late infantile neuronal ceroid lipofuscinosis
wt	wild-type
µg	microgram
µm	micrometer
sc	self-complementary

8. References

Adler, R. et al. (1979). Cholinergic neuronotrophic factors: intraocular distribution of trophic activity for ciliary neurons. Science 204(4400): 1434-1436.

Aiello, C. et al. (2009). Mutations in MFSD8/CLN7 are a frequent cause of variant-late infantile neuronal ceroid lipofuscinosis. Hum Mutat 30(3): E530-540.

Ait-Ali, N. et al. (2015). Rod-derived cone viability factor promotes cone survival by stimulating aerobic glycolysis. Cell 161(4): 817-832.

Aldahmesh, M. A. et al. (2009). Neuronal ceroid lipofuscinosis caused by MFSD8 mutations: a common theme emerging." Neurogenetics 10(4): 307-311.

Almasieh, M. et al. (2012). The molecular basis of retinal ganglion cell death in glaucoma. Prog Retin Eye Res 31(2): 152-181.

Arjunan, P. et al. (2018). VEGF-B is a potent antioxidant. Proc Natl Acad Sci U S A 115(41): 10351-10356.

Arrant, A. E. et al. (2018). Progranulin Gene Therapy Improves Lysosomal Dysfunction and Microglial Pathology Associated with Frontotemporal Dementia and Neuronal Ceroid Lipofuscinosis. J Neurosci 38(9): 2341-2358.

Arranz-Romera, A., M. Hernandez, P. Checa-Casalengua, A. Garcia-Layana, I. T. Molina-Martinez et al. (2021). A Safe GDNF and GDNF/BDNF Controlled Delivery System Improves Migration in Human Retinal Pigment Epithelial Cells and Survival in Retinal Ganglion Cells: Potential Usefulness in Degenerative Retinal Pathologies. Pharmaceuticals (Basel) 14(1).

Baranov, P. et al. (2017). A Novel Neuroprotective Small Molecule for Glial Cell Derived Neurotrophic Factor Induction and Photoreceptor Rescue. J Ocul Pharmacol Ther 33(5): 412-422.

Bartsch, U. et al. (2013). Apoptotic photoreceptor loss and altered expression of lysosomal proteins in the nclf mouse model of neuronal ceroid lipofuscinosis. Invest Ophthalmol Vis Sci 54(10): 6952-6959.

Bauwens, M. et al. (2020). Functional characterization of novel MFSD8 pathogenic variants anticipates neurological involvement in juvenile isolated maculopathy. Clin Genet 97(3): 426-436.

Birch, D. G. et al (2016). Long-term Follow-up of Patients With Retinitis Pigmentosa Receiving Intraocular Ciliary Neurotrophic Factor Implants. Am J Ophthalmol 170: 10-14.

Birch, D. G.et al. Ciliary Neurotrophic Factor Retinitis Pigmentosa Study (2013). Randomized trial of ciliary neurotrophic factor delivered by encapsulated cell intraocular implants for retinitis pigmentosa. Am J Ophthalmol 156(2): 283-292 e281.

Birtel, J. et al. (2018). Next-generation sequencing identifies unexpected genotype-phenotype correlations in patients with retinitis pigmentosa. PLoS

One 13(12): e0207958.
Bok, D. et al. (2002). Effects of adeno-associated virus-vectored ciliary neurotrophic factor on retinal structure and function in mice with a P216L rds/peripherin mutation. Exp Eye Res 74(6): 719-735.
Boustany, R. M. (2013). Lysosomal storage diseases--the horizon expands. Nat Rev Neurol 9(10): 583-598.
Brandenstein, L. et al. (2016). Lysosomal dysfunction and impaired autophagy in a novel mouse model deficient for the lysosomal membrane protein Cln7. Hum Mol Genet 25(4): 777-791.
Buch, P. K. et al. (2006). In contrast to AAV-mediated Cntf expression, AAV-mediated Gdnf expression enhances gene replacement therapy in rodent models of retinal degeneration. Mol Ther 14(5): 700-709.
Bush, R. A. et al. (2004). Encapsulated cell-based intraocular delivery of ciliary neurotrophic factor in normal rabbit: dose-dependent effects on ERG and retinal histology. Invest Ophthalmol Vis Sci 45(7): 2420-2430.
Byrne, A. M. et al. (2016). The synthetic progestin norgestrel acts to increase LIF levels in the rd10 mouse model of retinitis pigmentosa. Mol Vis 22: 264-274.
Cabrera-Salazar, M. A. et al. (2007). Timing of therapeutic intervention determines functional and survival outcomes in a mouse model of late infantile batten disease. Mol Ther 15(10): 1782-1788.
Carter-Dawson, L. D., M. M. LaVail (1979). Rods and cones in the mouse retina. I. Structural analysis using light and electron microscopy. J Comp Neurol 188(2): 245-262.
Carwile, M. E. et al. (1998). Rod outer segment maintenance is enhanced in the presence of bFGF, CNTF and GDNF. Exp Eye Res 66(6): 791-805.
Cayouette, M. et al. (1998). Intraocular gene transfer of ciliary neurotrophic factor prevents death and increases responsiveness of rod photoreceptors in the retinal degeneration slow mouse. J Neurosci 18(22): 9282-9293.
Cayouette, M., C. Gravel (1997). Adenovirus-mediated gene transfer of ciliary neurotrophic factor can prevent photoreceptor degeneration in the retinal degeneration (rd) mouse. Hum Gene Ther 8(4): 423-430.
Chang, M. et al. (2008). Intraventricular enzyme replacement improves disease phenotypes in a mouse model of late infantile neuronal ceroid lipofuscinosis. Mol Ther 16(4): 649-656.
Checa-Casalengua, P. et al. (2011). Retinal ganglion cells survival in a glaucoma model by GDNF/Vit E PLGA microspheres prepared according to a novel microencapsulation procedure. J Control Release 156(1): 92-100.
Chen, X. et al. (2022). AAV9/MFSD8 gene therapy is effective in preclinical models of neuronal ceroid lipofuscinosis type 7 disease. J Clin Invest.
Chew, E. Y. et al. Macular Telangiectasia Type 2-Phase (2019). Effect of Ciliary Neurotrophic Factor on Retinal Neurodegeneration in Patients with Macular Telangiectasia Type 2: A Randomized Clinical Trial. Ophthalmology 126(4): 540-549.

Chong, N. H. et al. (1999). Repeated injections of a ciliary neurotrophic factor analogue leading to long-term photoreceptor survival in hereditary retinal degeneration. Invest Ophthalmol Vis Sci 40(6): 1298-1305.
Conti, L. et al. (2005). Niche-independent symmetrical self-renewal of a mammalian tissue stem cell. PLoS Biol 3(9): e283.
Craiu, D. et al. (2015). Rett-like onset in late-infantile neuronal ceroid lipofuscinosis (CLN7) caused by compound heterozygous mutation in the MFSD8 gene and review of the literature data on clinical onset signs. Eur J Paediatr Neurol 19(1): 78-86.
Cuenca, N. et al. (2014). Cellular responses following retinal injuries and therapeutic approaches for neurodegenerative diseases. Prog Retin Eye Res 43: 17-75.
Dalkara, D. et al. (2011). AAV mediated GDNF secretion from retinal glia slows down retinal degeneration in a rat model of retinitis pigmentosa. Mol Ther 19(9): 1602-1608.
Damme, M. et al. (2014). Gene disruption of Mfsd8 in mice provides the first animal model for CLN7 disease. Neurobiol Dis 65: 12-24.
Del Rio, P. et al. (2011). GDNF-induced osteopontin from Muller glial cells promotes photoreceptor survival in the Pde6brd1 mouse model of retinal degeneration. Glia 59(5): 821-832.
Dolisca, S. B. et al. (2013). Batten disease: clinical aspects, molecular mechanisms, translational science, and future directions. J Child Neurol 28(9): 1074-1100.
Dulz, S. et al. (2020). Intravitreal Co-Administration of GDNF and CNTF Confers Synergistic and Long-Lasting Protection against Injury-Induced Cell Death of Retinal Ganglion Cells in Mice. Cells 9(9).
Ejstrup, R. et al. (2010). Pharmacokinetics of intravitreal glial cell line-derived neurotrophic factor: experimental studies in pigs. Exp Eye Res 91(6): 890-895.
Emerich, D. F., C. G. Thanos (2008). NT-501: an ophthalmic implant of polymer-encapsulated ciliary neurotrophic factor-producing cells. Curr Opin Mol Ther 10(5): 506-515.
Fischer, D., M. Leibinger (2012). Promoting optic nerve regeneration. Prog Retin Eye Res 31(6): 688-701.
Flachsbarth, K. et al. (2018). Pronounced synergistic neuroprotective effect of GDNF and CNTF on axotomized retinal ganglion cells in the adult mouse. Exp Eye Res 176: 258-265.
Flachsbarth, K. et al. (2014). Neural stem cell-based intraocular administration of ciliary neurotrophic factor attenuates the loss of axotomized ganglion cells in adult mice. Invest Ophthalmol Vis Sci 55(11): 7029-7039.
Frasson, M. et al. (1999). Glial cell line-derived neurotrophic factor induces histologic and functional protection of rod photoreceptors in the rd/rd mouse. Invest Ophthalmol Vis Sci 40(11): 2724-2734.
Gamm, D. M. et al. (2007). Protection of visual functions by human neural

progenitors in a rat model of retinal disease. PLoS One 2(3): e338.
Garcia-Caballero, C. et al. (2018). Photoreceptor preservation induced by intravitreal controlled delivery of GDNF and GDNF/melatonin in rhodopsin knockout mice. Mol Vis 24: 733-745.
Gardner, E., S. E. Mole (2021). The Genetic Basis of Phenotypic Heterogeneity in the Neuronal Ceroid Lipofuscinoses. Front Neurol 12: 754045.
Gargini, C. et al. (1999). The impact of basic fibroblast growth factor on photoreceptor function and morphology. Invest Ophthalmol Vis Sci 40(9): 2088-2099.
Ghasemi, M. et al. (2018). Ciliary neurotrophic factor (CNTF) delivery to retina: an overview of current research advancements. Artif Cells Nanomed Biotechnol 46(8): 1694-1707.
Glaser, T. et al. (2007). Tripotential differentiation of adherently expandable neural stem (NS) cells. PLoS One 2(3): e298.
Gregory-Evans, K. et al. (2009). Ex vivo gene therapy using intravitreal injection of GDNF-secreting mouse embryonic stem cells in a rat model of retinal degeneration. Mol Vis 15: 962-973.
Griffey, M. et al. (2004). Adeno-associated virus 2-mediated gene therapy decreases autofluorescent storage material and increases brain mass in a murine model of infantile neuronal ceroid lipofuscinosis. Neurobiol Dis 16(2): 360-369.
Griffey, M. et al. (2005). AAV2-mediated ocular gene therapy for infantile neuronal ceroid lipofuscinosis. Mol Ther 12(3): 413-421.
Griffey, M. A. et al. (2006). CNS-directed AAV2-mediated gene therapy ameliorates functional deficits in a murine model of infantile neuronal ceroid lipofuscinosis. Mol Ther 13(3): 538-547.
Hackett, S. F. et al. (1997). Neurotrophic factors, cytokines and stress increase expression of basic fibroblast growth factor in retinal pigmented epithelial cells. Exp Eye Res 64(6): 865-873.
Haltia, M., H. H. Goebel (2013). The neuronal ceroid-lipofuscinoses: a historical introduction. Biochim Biophys Acta 1832(11): 1795-1800.
Harada, C., T. Harada, H. M. Quah, F. Maekawa, K. Yoshida, S. Ohno, K. Wada, L. F. Parada, K. Tanaka (2003). Potential role of glial cell line-derived neurotrophic factor receptors in Muller glial cells during light-induced retinal degeneration. Neuroscience 122(1): 229-235.
Harada, T. et al. (2002). Microglia-Muller glia cell interactions control neurotrophic factor production during light-induced retinal degeneration. J Neurosci 22(21): 9228-9236.
Hauck, S. M. et al. (2006). GDNF family ligands trigger indirect neuroprotective signaling in retinal glial cells. Mol Cell Biol 26(7): 2746-2757.
Hellstrom, M. et al. (2011). Negative impact of rAAV2 mediated expression of SOCS3 on the regeneration of adult retinal ganglion cell axons. Mol Cell Neurosci 46(2): 507-515.

Hellstrom, M., M. A. Pollett, A. R. Harvey (2011). Post-injury delivery of rAAV2-CNTF combined with short-term pharmacotherapy is neuroprotective and promotes extensive axonal regeneration after optic nerve trauma. J Neurotrauma 28(12): 2475-2483.
Hosseini Bereshneh, A., M. Garshasbi (2018). Novel in-frame deletion in MFSD8 gene revealed by trio whole exome sequencing in an Iranian affected with neuronal ceroid lipofuscinosis type 7: a case report. J Med Case Rep 12(1): 281.
Hu, J. et al. (2012). Intravenous high-dose enzyme replacement therapy with recombinant palmitoyl-protein thioesterase reduces visceral lysosomal storage and modestly prolongs survival in a preclinical mouse model of infantile neuronal ceroid lipofuscinosis. Mol Genet Metab 107(1-2): 213-221.
Hu, Z. L. et al. (2017). Neuroprotective effects of BDNF and GDNF in intravitreally transplanted mesenchymal stem cells after optic nerve crush in mice. Int J Ophthalmol 10(1): 35-42.
Huang, S. P. et al. (2004). Intraocular gene transfer of ciliary neurotrophic factor rescues photoreceptor degeneration in RCS rats. J Biomed Sci 11(1): 37-48.
Ishikawa, H. et al. (2005). Effect of GDNF gene transfer into axotomized retinal ganglion cells using in vivo electroporation with a contact lens-type electrode. Gene Ther 12(4): 289-298.
Jankowiak, W. et al. (2016). Retinal Degeneration in Mice Deficient in the Lysosomal Membrane Protein CLN7. Invest Ophthalmol Vis Sci 57(11): 4989-4998.
Jankowiak, W. et al. (2015). Sustained Neural Stem Cell-Based Intraocular Delivery of CNTF Attenuates Photoreceptor Loss in the nclf Mouse Model of Neuronal Ceroid Lipofuscinosis. PLoS One 10(5): e0127204.
Ji, J. Z. et al. (2004). CNTF promotes survival of retinal ganglion cells after induction of ocular hypertension in rats: the possible involvement of STAT3 pathway. Eur J Neurosci 19(2): 265-272.
Jiang, C. et al. (2007). Intravitreal injections of GDNF-loaded biodegradable microspheres are neuroprotective in a rat model of glaucoma. Mol Vis 13: 1783-1792.
Jing, S. et al. (1996). GDNF-induced activation of the ret protein tyrosine kinase is mediated by GDNFR-alpha, a novel receptor for GDNF. Cell 85(7): 1113-1124.
Joly, S. et al. (2008). Leukemia inhibitory factor extends the lifespan of injured photoreceptors in vivo. J Neurosci 28(51): 13765-13774.
Jomary, C. et al. (1999). Expression patterns of neurturin and its receptor components in developing and degenerative mouse retina. Invest Ophthalmol Vis Sci 40(3): 568-574.
Jung, G. et al. (2013). Genetically modified neural stem cells for a local and sustained delivery of neuroprotective factors to the dystrophic mouse retina. Stem Cells Transl Med 2(12): 1001-1010.

Katz, M. L. et al. (2014). Enzyme replacement therapy attenuates disease progression in a canine model of late-infantile neuronal ceroid lipofuscinosis (CLN2 disease). J Neurosci Res 92(11): 1591-1598.
Katz, M. L. et al. (2015). AAV gene transfer delays disease onset in a TPP1-deficient canine model of the late infantile form of Batten disease. Sci Transl Med 7(313): 313ra180.
Kauper, K. et al. (2012). Two-year intraocular delivery of ciliary neurotrophic factor by encapsulated cell technology implants in patients with chronic retinal degenerative diseases. Invest Ophthalmol Vis Sci 53(12): 7484-7491.
Khan, K. N. et al. (2017). Specific Alleles of CLN7/MFSD8, a Protein That Localizes to Photoreceptor Synaptic Terminals, Cause a Spectrum of Nonsyndromic Retinal Dystrophy. Invest Ophthalmol Vis Sci 58(7): 2906-2914.
Kirsch, M. et al. (1997). Evidence for multiple, local functions of ciliary neurotrophic factor (CNTF) in retinal development: expression of CNTF and its receptors and in vitro effects on target cells. J Neurochem 68(3): 979-990.
Klein, A. et al. (1994). Sphingolipid activator protein D (sap-D) stimulates the lysosomal degradation of ceramide in vivo. Biochem Biophys Res Commun 200(3): 1440-1448.
Kleine Holthaus, S. M. et al. (2018). Prevention of Photoreceptor Cell Loss in a Cln6(nclf) Mouse Model of Batten Disease Requires CLN6 Gene Transfer to Bipolar Cells. Mol Ther 26(5): 1343-1353.
Klionsky, D. J. et al. (2021). Guidelines for the use and interpretation of assays for monitoring autophagy (4th edition)(1). Autophagy 17(1): 1-382.
Klocker, N. et al. (1997). In vivo neurotrophic effects of GDNF on axotomized retinal ganglion cells. Neuroreport 8(16): 3439-3442.
Koeberle, P. D.,A. K. Ball (1998). Effects of GDNF on retinal ganglion cell survival following axotomy. Vision Res 38(10): 1505-1515.
Koeberle, P. D., A. K. Ball (2002). Neurturin enhances the survival of axotomized retinal ganglion cells in vivo: combined effects with glial cell line-derived neurotrophic factor and brain-derived neurotrophic factor. Neuroscience 110(3): 555-567.
Kohlschutter, A. et al. (2019). Current and Emerging Treatment Strategies for Neuronal Ceroid Lipofuscinoses. CNS Drugs 33(4): 315-325.
Kolomeyer, A. M., M. A. Zarbin (2014). Trophic factors in the pathogenesis and therapy for retinal degenerative diseases. Surv Ophthalmol 59(2): 134-165.
Kousi, M. et al. (2009). Mutations in CLN7/MFSD8 are a common cause of variant late-infantile neuronal ceroid lipofuscinosis. Brain 132(Pt 3): 810-819.
Kozina, A. A., E. G. Okuneva, N. V. Baryshnikova, A. Y. Krasnenko, K. Y. Tsukanov et al. (2018). A novel MFSD8 mutation in a Russian patient with neuronal ceroid lipofuscinosis type 7: a case report. BMC Med Genet 19(1): 151.
Kurokawa, T. et al. (1999). BDNF diminishes caspase-2 but not c-Jun

immunoreactivity of neurons in retinal ganglion cell layer after transient ischemia. Invest Ophthalmol Vis Sci 40(12): 3006-3011.
Kuse, Y. et al. (2017). Progranulin deficiency causes the retinal ganglion cell loss during development. Sci Rep 7(1): 1679.
Langlo, C. et al. (2015). CNGB3-Achromatopsia Clinical Trial With CNTF: Diminished Rod Pathway Responses With No Evidence of Improvement in Cone Function. Invest Ophthalmol Vis Sci 56(3): 1505.
Lau, D. et al. (2000). Retinal degeneration is slowed in transgenic rats by AAV-mediated delivery of FGF-2. Invest Ophthalmol Vis Sci 41(11): 3622-3633.
LaVail et al. (1992). Multiple growth factors, cytokines, and neurotrophins rescue photoreceptors from the damaging effects of constant light. Proc Natl Acad Sci U S A 89(23): 11249-11253.
LaVail et al. (1998). Protection of mouse photoreceptors by survival factors in retinal degenerations. Invest Ophthalmol Vis Sci 39(3): 592-602.
Lawrence, J. M. et al. (2004). Transplantation of Schwann cell line clones secreting GDNF or BDNF into the retinas of dystrophic Royal College of Surgeons rats. Invest Ophthalmol Vis Sci 45(1): 267-274.
Leaver, S. G. et al. (2006). AAV-mediated expression of CNTF promotes long-term survival and regeneration of adult rat retinal ganglion cells. Gene Ther 13(18): 1328-1341.
Liang, F. Q. et al. (2001). Long-term protection of retinal structure but not function using RAAV.CNTF in animal models of retinitis pigmentosa. Mol Ther 4(5): 461-472.
Liang, F. Q. et al. (2001). AAV-mediated delivery of ciliary neurotrophic factor prolongs photoreceptor survival in the rhodopsin knockout mouse. Mol Ther 3(2): 241-248.
Lin, L. F. et al. (1993). GDNF: a glial cell line-derived neurotrophic factor for midbrain dopaminergic neurons. Science 260(5111): 1130-1132.
Lipinski, D. M., A. R. Barnard, M. S. Singh, C. Martin, E. J. Lee, W. I. L. Davies, R. E. MacLaren (2015). CNTF Gene Therapy Confers Lifelong Neuroprotection in a Mouse Model of Human Retinitis Pigmentosa. Mol Ther 23(8): 1308-1319.
Lipinski, D. M. et al. (2011). Assessment of cone survival in response to CNTF, GDNF, and VEGF165b in a novel ex vivo model of end-stage retinitis pigmentosa. Invest Ophthalmol Vis Sci 52(10): 7340-7346.
Liu, J. et al. (2022). Intravitreal gene therapy restores the autophagy-lysosomal pathway and attenuates retinal degeneration in cathepsin D-deficient mice. Neurobiol Dis 164: 105628.
Lopez-Fabuel, I. et al. (2022). Aberrant upregulation of the glycolytic enzyme PFKFB3 in CLN7 neuronal ceroid lipofuscinosis. Nat Commun 13(1): 536.
Lu, J. Y. et al. (2015). Intrathecal enzyme replacement therapy improves motor function and survival in a preclinical mouse model of infantile neuronal ceroid lipofuscinosis. Mol Genet Metab 116(1-2): 98-105.

Macauley, S. L. et al. (2012). Synergistic effects of central nervous system-directed gene therapy and bone marrow transplantation in the murine model of infantile neuronal ceroid lipofuscinosis. Ann Neurol 71(6): 797-804.
MacDonald, I. M. et al. (2007). Preventing blindness in retinal disease: ciliary neurotrophic factor intraocular implants. Can J Ophthalmol 42(3): 399-402.
Magliyah, M. et al. (2019). Multimodal retinal imaging in MFSD8-neuronal ceroid lipofuscinosis. Ophthalmic Genet 40(6): 588-590.
Marques, A. R. A. et al. (2020). Enzyme replacement therapy with recombinant pro-CTSD (cathepsin D) corrects defective proteolysis and autophagy in neuronal ceroid lipofuscinosis. Autophagy 16(5): 811-825.
McGee Sanftner, L. H. et al. (2001). Glial cell line derived neurotrophic factor delays photoreceptor degeneration in a transgenic rat model of retinitis pigmentosa. Mol Ther 4(6): 622-629.
McGill, T. J. et al. (2007). Intraocular CNTF reduces vision in normal rats in a dose-dependent manner. Invest Ophthalmol Vis Sci 48(12): 5756-5766.
Mei, X., A. Chaffiol, C. Kole, Y. Yang, G. Millet-Puel, E. Clerin, N. Ait-Ali, J. Bennett et al. (2016). The Thioredoxin Encoded by the Rod-Derived Cone Viability Factor Gene Protects Cone Photoreceptors Against Oxidative Stress. Antioxid Redox Signal 24(16): 909-923.
Mirza, M. et al. (2013). Progressive retinal degeneration and glial activation in the CLN6 (nclf) mouse model of neuronal ceroid lipofuscinosis: a beneficial effect of DHA and curcumin supplementation. PLoS One 8(10): e75963.
Mole, S. E., S. L. Cotman (2015). Genetics of the neuronal ceroid lipofuscinoses (Batten disease). Biochim Biophys Acta 1852(10 Pt B): 2237-2241.
Nita, D. A. et al. (2016). Neuronal ceroid lipofuscinoses. Epileptic Disord 18(S2): 73-88.
Ohnaka, M. et al. (2012). Long-term expression of glial cell line-derived neurotrophic factor slows, but does not stop retinal degeneration in a model of retinitis pigmentosa. J Neurochem 122(5): 1047-1053.
Patino, L. C. et al. (2014). Exome sequencing is an efficient tool for variant late-infantile neuronal ceroid lipofuscinosis molecular diagnosis. PLoS One 9(10): e109576.
Peachey, N. S. et al. (1993). Properties of the mouse cone-mediated electroretinogram during light adaptation. Neurosci Lett 162(1-2): 9-11.
Pernet, V., S. Joly, D. Dalkara, N. Jordi, O. Schwarz, F. Christ, D. V. Schaffer, J. G. Flannery, M. E. Schwab (2013). Long-distance axonal regeneration induced by CNTF gene transfer is impaired by axonal misguidance in the injured adult optic nerve. Neurobiol Dis 51: 202-213.
Politi, L. E. et al. (2001). Effect of GDNF on neuroblast proliferation and photoreceptor survival: additive protection with docosahexaenoic acid. Invest Ophthalmol Vis Sci 42(12): 3008-3015.
Pollard, S. M. et al. (2006). Adherent neural stem (NS) cells from fetal and adult forebrain. Cereb Cortex 16 Suppl 1: i112-120.

Poncet, A. F. et al. (2022). Contribution of Whole-Genome Sequencing and Transcript Analysis to Decipher Retinal Diseases Associated with MFSD8 Variants. Int J Mol Sci 23(8).
Read, S. P. et al. (2010). POD nanoparticles expressing GDNF provide structural and functional rescue of light-induced retinal degeneration in an adult mouse. Mol Ther 18(11): 1917-1926.
Reith, M. et al. (2022). A Novel, Apparently Silent Variant in MFSD8 Causes Neuronal Ceroid Lipofuscinosis with Marked Intrafamilial Variability. Int J Mol Sci 23(4).
Rhee, K. D. et al. (2013). CNTF-mediated protection of photoreceptors requires initial activation of the cytokine receptor gp130 in Muller glial cells. Proc Natl Acad Sci U S A 110(47): E4520-4529.
Rhee, K. D. et al. (2007). Molecular and cellular alterations induced by sustained expression of ciliary neurotrophic factor in a mouse model of retinitis pigmentosa. Invest Ophthalmol Vis Sci 48(3): 1389-1400.
Richardson, P. M. (1994). Ciliary neurotrophic factor: a review. Pharmacol Ther 63(2): 187-198.
Roosing, S. et al. (2015). Mutations in MFSD8, encoding a lysosomal membrane protein, are associated with nonsyndromic autosomal recessive macular dystrophy. Ophthalmology 122(1): 170-179.
Sanicola, M. et al. (1997). Glial cell line-derived neurotrophic factor-dependent RET activation can be mediated by two different cell-surface accessory proteins. Proc Natl Acad Sci U S A 94(12): 6238-6243.
Schlichtenbrede, F. C. et al. (2003). Intraocular gene delivery of ciliary neurotrophic factor results in significant loss of retinal function in normal mice and in the Prph2Rd2/Rd2 model of retinal degeneration. Gene Ther 10(6): 523-527.
Schmeer, C. et al. (2002). Dose-dependent rescue of axotomized rat retinal ganglion cells by adenovirus-mediated expression of glial cell-line derived neurotrophic factor in vivo. Eur J Neurosci 15(4): 637-643.
Shevtsova, Z. et al. (2010). CNS-expressed cathepsin D prevents lymphopenia in a murine model of congenital neuronal ceroid lipofuscinosis. Am J Pathol 177(1): 271-279.
Shyng, C. et al. (2017). Synergistic effects of treating the spinal cord and brain in CLN1 disease. Proc Natl Acad Sci U S A 114(29): E5920-E5929.
Sieving, P. A. et al. (2006). Ciliary neurotrophic factor (CNTF) for human retinal degeneration: phase I trial of CNTF delivered by encapsulated cell intraocular implants. Proc Natl Acad Sci U S A 103(10): 3896-3901.
Soldati, C. et al. (2021). Repurposing of tamoxifen ameliorates CLN3 and CLN7 disease phenotype. EMBO Mol Med 13(10): e13742.
Takahashi, M., G. M. Cooper (1987). ret transforming gene encodes a fusion protein homologous to tyrosine kinases. Mol Cell Biol 7(4): 1378-1385.
Takahata, K., H. Katsuki, T. Kume, D. Nakata, K. Ito, S. Muraoka, F. Yoneda, S. Kashii et al. (2003). Retinal neuronal death induced by intraocular

administration of a nitric oxide donor and its rescue by neurotrophic factors in rats. Invest Ophthalmol Vis Sci 44(4): 1760-1766.
Talcott, K. E. et al. (2011). Longitudinal study of cone photoreceptors during retinal degeneration and in response to ciliary neurotrophic factor treatment. Invest Ophthalmol Vis Sci 52(5): 2219-2226.
Tao, W. et al. (2002). Encapsulated cell-based delivery of CNTF reduces photoreceptor degeneration in animal models of retinitis pigmentosa. Invest Ophthalmol Vis Sci 43(10): 3292-3298.
Thanos, C. G. et al. (2004). Sustained secretion of ciliary neurotrophic factor to the vitreous, using the encapsulated cell therapy-based NT-501 intraocular device. Tissue Eng 10(11-12): 1617-1622.
Topcu, M. et al. (2004). Evaluation of 36 patients from Turkey with neuronal ceroid lipofuscinosis: clinical, neurophysiological, neuroradiological and histopathologic studies. Turk J Pediatr 46(1): 1-10.
Touchard, E. et al. (2012). Non-viral gene therapy for GDNF production in RCS rat: the crucial role of the plasmid dose. Gene Ther 19(9): 886-898.
Treanor, J. J. et al. (1996). Characterization of a multicomponent receptor for GDNF. Nature 382(6586): 80-83.
Trupp, M. et al. (1999). Ret-dependent and -independent mechanisms of glial cell line-derived neurotrophic factor signaling in neuronal cells. J Biol Chem 274(30): 20885-20894.
Valiente-Soriano, F. J. et al. (2019). Topical Brimonidine or Intravitreal BDNF, CNTF, or bFGF Protect Cones Against Phototoxicity. Transl Vis Sci Technol 8(6): 36.
van Adel, B. A. et al. (2005). Ciliary neurotrophic factor protects retinal ganglion cells from axotomy-induced apoptosis via modulation of retinal glia in vivo. J Neurobiol 63(3): 215-234.
Varon, S. et al. (1979). Cholinergic neuronotrophic factors: I. Survival, neurite outgrowth and choline acetyltransferase activity in monolayer cultures from chick embryo ciliary ganglia. Brain Res 173(1): 29-45.
Vidal-Sanz, M. et al. (2001). Brimonidine's neuroprotective effects against transient ischaemia-induced retinal ganglion cell death. Eur J Ophthalmol 11 Suppl 2: S36-40.
Vuillemenot, B. R. et al. (2015). Nonclinical evaluation of CNS-administered TPP1 enzyme replacement in canine CLN2 neuronal ceroid lipofuscinosis. Mol Genet Metab 114(2): 281-293.
Wahlberg, L. U. et al. (2020). Long-term, stable, targeted biodelivery and efficacy of GDNF from encapsulated cells in the rat and Goettingen miniature pig brain. Curr Res Pharmacol Drug Discov 1: 19-29.
Wang, Y. et al. (2021). CLN7 is an organellar chloride channel regulating lysosomal function. Sci Adv 7(51): eabj9608.
Ward, M. S. et al. (2007). Neuroprotection of retinal ganglion cells in DBA/2J mice with GDNF-loaded biodegradable microspheres. J Pharm Sci 96(3): 558-568.

Wen, R. et al. (2006). Regulation of rod phototransduction machinery by ciliary neurotrophic factor. J Neurosci 26(52): 13523-13530.
Wen, R. et al. (2012). CNTF and retina." Prog Retin Eye Res 31(2): 136-151.
Whiting, R. E., K. Narfstrom, G. Yao, J. W. Pearce, J. R. Coates, L. J. Castaner, C. A. Jensen et al. (2014). Enzyme replacement therapy delays pupillary light reflex deficits in a canine model of late infantile neuronal ceroid lipofuscinosis. Exp Eye Res 125: 164-172.
Whiting, R. E. et al. (2015). Multifocal retinopathy in Dachshunds with CLN2 neuronal ceroid lipofuscinosis. Exp Eye Res 134: 123-132.
Whiting, R. E. H. et al. (2020). Intravitreal enzyme replacement preserves retinal structure and function in canine CLN2 neuronal ceroid lipofuscinosis. Exp Eye Res 197: 108130.
Whiting, R. E. H. et al. (2020). Intravitreal enzyme replacement inhibits progression of retinal degeneration in canine CLN2 neuronal ceroid lipofuscinosis. Exp Eye Res 198: 108135.
Wilson, A. M., A. Di Polo (2012). Gene therapy for retinal ganglion cell neuroprotection in glaucoma. Gene Ther 19(2): 127-136.
Wong, F. S. et al. (2016). Sustained Delivery of Bioactive GDNF from Collagen, Alginate-Based Cell-Encapsulating Gel Promoted Photoreceptor Survival in an Inherited Retinal Degeneration Model. PLoS One 11(7): e0159342.
Wong, F. S. Y. et al. (2017). Delivery of therapeutics to posterior eye segment: cell-encapsulating systems. Neural Regen Res 12(4): 576-577.
Wu, W. C. et al. (2002). Gene therapy for detached retina by adeno-associated virus vector expressing glial cell line-derived neurotrophic factor. Invest Ophthalmol Vis Sci 43(11): 3480-3488.
Xiang, Q. et al. (2021). Novel MFSD8 Variants in a Chinese Family with Nonsyndromic Macular Dystrophy. J Ophthalmol 2021: 6684045.
Xie, J. X. et al. (2015). Positive effects of bFGF modified rat amniotic epithelial cells transplantation on transected rat optic nerve. PLoS One 10(3): e0119119.
Yan, Q. et al. (1999). Glial cell line-derived neurotrophic factor (GDNF) promotes the survival of axotomized retinal ganglion cells in adult rats: comparison to and combination with brain-derived neurotrophic factor (BDNF). J Neurobiol 38(3): 382-390.
Zare-Abdollahi, D. et al. (2019). MFSD8 gene mutations; evidence for phenotypic heterogeneity. Ophthalmic Genet 40(2): 141-145.
Zein, W. M. et al. (2014). CNGB3-achromatopsia clinical trial with CNTF: diminished rod pathway responses with no evidence of improvement in cone function. Invest Ophthalmol Vis Sci 55(10): 6301-6308.
Zhang, K. et al. (2011). Ciliary neurotrophic factor delivered by encapsulated cell intraocular implants for treatment of geographic atrophy in age-related macular degeneration. Proc Natl Acad Sci U S A 108(15): 6241-6245.
Zhang, S. et al. (2012). Enhancement of rAAV2-mediated transgene

expression in retina cells in vitro and in vivo by coadministration of low-dose chemotherapeutic drugs. Invest Ophthalmol Vis Sci 53(6): 2675-2684.
Zheng, K. et al. (2018). Ciliary Neurotrophic Factor (CNTF) Protects Myocardial Cells from Oxygen Glucose Deprivation (OGD)/Re-Oxygenation via Activation of Akt-Nrf2 Signaling. Cell Physiol Biochem 51(4): 1852-1862.
Zhou, Y. et al. (2020). Sulforaphane-cysteine inhibited migration and invasion via enhancing mitophagosome fusion to lysosome in human glioblastoma cells. Cell Death Dis 11(9): 819.

9. Declaration of personal contributions to the thesis

Title: Stem cell-based intravitreal delivery of GDNF and CNTF for the treatment of retinal degeneration in a mouse model of CLN7 disease

Description of personal contribution:

1. support of animal experiments
2. preparation, freezing and cryostat sectioning of retinas
3. immunohistochemistry of retinal sections
4. fluorescence microscopy checking
5. imaging of retinal sections (ApoTome2)
6. pin and fixation of lens
7. imaging of lens (confocal microscope)
8. qualitative evaluation of immunostained retina sections
9. collecting ERG data and analysis
10. figures preparation
11. statistical analyses
12. support of manuscript draft preparation

10. Acknowledgements

First of all, I can hardly express my truehearted appreciation to my supervisor, Professor Dr. Udo Bartsch, for giving me this precious opportunity to perform my doctoral study in his lab and for providing different but meaningful research projects. He always has an opened door of his office. That is priceless access for Whoever has problems or perplexity. He devoted himself to scientific research. I appreciate it a lot that he has such an incomparable passion or enthusiasm for science. I can't thank enough for him helping me from green hands to a research staff member who could create a big blueprint for the scientific projects. The process of changing can be long and arduous, thanks for putting up with me and my innocence.

I would like to give special thanks to my colleagues Elke Becker, Sabine Helbing and Stefanie Schlichting for the contribution of their fantastic technical assistance. Thank you all for teaching me all the experimental methods with patience and enthusiasm.

Many thanks to Mia and Crystal, who kindly helped me a lot with both my project and my private life. I am glad to have you two angels keep me company in Germany. Thanks to Mahmoud Bassal for teaching me with imaging and analysis, Lynn Michelle for helping me with statistical analysis problems, Yevgeniya Atiskova and Susanne Bartsch for showing me how to perform ERG and solve ERG problems.

I am also deeply indebted to China Scholarship Council for offering me the opportunity and the scholarship for my doctoral study in Germany. In addition, I would like to thank the Chinese Embassy in Germany for their effort to support emergency supplies to students during Corona time.

I would like to offer my sincere thanks to Yonghao Gu, who gave me treasured suggestion and encouragement for my daily routine in the hospital and my master's study.

I am especially grateful for my close friends who play an important role in my colorful life in China and Germany.

I avail myself of this precious opportunity to express my heartfelt thanks to my boyfriend Xu Zhu for his unconditional love and support. Thanks for each necessary compromise he made to this relationship. I appreciate it a lot.

Finally, I would like to thank my beloved parents and sister for endless love and financial support. Thanks to my uncle and aunt for providing me both financial support and excellent advice for life. I have boldness to pursue my dreams only because I know that you would cover my back all the time.

11. Curriculum vitae

Lebenslauf wurde aus datenschutzrechtlichen Gründen entfernt.

12. Eidesstattliche Versicherung

Ich versichere ausdrücklich, dass ich die Arbeit selbständig und ohne fremde Hilfe verfasst, andere als die von mir angegebenen Quellen und Hilfsmittel nicht benutzt und die aus den benutzten Werken wörtlich oder inhaltlich entnommenen Stellen einzeln nach Ausgabe (Auflage und Jahr des Erscheinens), Band und Seite des benutzten Werkes kenntlich gemacht habe.
Ferner versichere ich, dass ich die Dissertation bisher nicht einem Fachvertreter an einer anderen Hochschule zur Überprüfung vorgelegt oder mich anderweitig um Zulassung zur Promotion beworben habe.
Ich erkläre mich einverstanden, dass meine Dissertation vom Dekanat der Medizinischen Fakultät mit einer gängigen Software zur Erkennung von Plagiaten überprüft werden kann.

Unterschrift:

Xingying Wei 02.08.2022